
Hurghada
Quesir
Marsa
Alam
Eastern Desert Field Workshop
Feb. 18-23, 2007
Hurghada, Quesir, and Marsa Alam

Eastern Desert of Egypt 2007 Field Conference

PARTICIPANTS	E-Mail
1- Dr. Victoria Pease (Stockholm University)	vicky.pease@geo.su.se
2- Dr. Martin Whitehouse (Swedish Museum of Natural History)	martin.whitehouse@nrm.se
3- Dr. Simon Wilde (Curtin University)	S.Wilde@curtin.edu.au
4- Dr. Robert Stern (U. Texas at Dallas)	rjstern@utdallas.edu
5- Dr. Ian Pitcairn (Stockholm University)	pitcairn@geol.queensu.ca
6- Dr. Osama Kaseem (National Research Center, Egypt)	kassemo1@yahoo.com
7- Dr. Hani Shalaby (Nuclear Materials Corporation, Egypt)	prhanishalaby@yahoo.com
8- Mr. Kamal Ali (U. Texas at Dallas)	kaa042000@utdallas.edu
9- Dr. Cees W. Passchier (Johannes Gutenberg Universität)	cpasschi@uni-mainz.de
10- Mr. Hossam Khamis (Nuclear Materials Corp., Egypt)	hakhamis3@yahoo.com
11- Dr. Arild Andressen (Univerisity of Oslo, Norway)	arild.andresen@geologi.uio.no
12- Dr. Ghaleb Jarrar (University of Jordan)	jarrargh@ju.edu.jo
13- Mr. Anwar Farasani (SGS)	farasani.AA@sgs.org.sa
14- Dr. Peter R. Johnson (SGS)	Johnson.PR@sgs.org.sa
15- Dr. Wieslaw Kozdroj (SGS)	wieslaw.kozdroj@pgi.gov.pl
16- Mr. Fayek Kattan (SGS)	Kattan.FH@sgs.org.sa
17- Mr. Saad Al Garny (SGS)	garni.SM@sgs.org.sa
18- Mr. Adeen Al- Hussaini (SGS)	barkati.AN@sgs.org.sa
29- Mr. Mohamed al Kaff (SGS)	kaff.MH@sgs.org.sa

19 participants from 8 countries

SCHEDULE OF ACTIVITIES

NED = North Eastern Desert, CED= Central Eastern Desert; SED = South Eastern Desert

17 Feb., Sat. - arrive Hurghada (overnight Hurghada)

18 Feb., Sun - Travel to Quesir. Stop en route for **field trip NED/CED boundary**: Qena-Safaga road traverse. Examine ~600-670 Ma grantitic rocks and intrusive relationships (overnight Quesir).

19 Feb., Mon. - **Field trip CED**: Qena-Quesir road traverse, including ~610 Ma Meatiq dome, ~600 Fawkhir A-type granite and Fawkhir ophiolite, and ~600 Ma Hammamat sediments (overnight Quesir).

20 Feb., Tues. - **Field trip CED**: Wadi Kareim and Wadi Dabbagh: ~750 Ma metavolcanics, diamictite and BIF (overnight Marsa Alum).

21 Feb., Wed. - **Field trip CED-SED boundary**: Marsa Alam mixed magmas OR Wadi El Gimal - Zabara district; berylliferous zone between mylonitized biotite granite and ophiolitic melange, as well as Mo and Sn

mineralization. This is the northwestern part of the southern Precambrian shield (overnight Marsa Alum).

22 Feb., Thurs.- **Field trip NED:** G. Qattar-Dokhan area (west of Hurghada), examine ~600Ma A-type granite, Dokhan volcanics, Hammamat sediments, and bimodal dike swarms (overnight Hurghada).

23 Feb., Fri. - **Workshop**, am=presentations; pm=discussions (overnight Hurghada).

24 Feb., Sat. - depart Hurghada

VISAS

European and US citizens can obtain visas from Egyptian consulates abroad or upon their arrival to Egypt. Saudis and Jordanians are exempt from needing visas for Egypt. Please find below the web-site which shows the requirements for getting visa in case some would like to have it before travel.

http://www.roadtoegypt.com/information/visas_passports.htm

HOTELS

1. Roma Hotel - Hurghada
http://travel.hotels-and-discounts.com/index.jsp?pageName=hotInfo&cid=59562&hotelID=235832&city=&stateProvince=&country=&hotel=01

2. Equinex El Nabaa – Marsa Alam
http://memphistours.com/Egyptian_hotels_detials.php?Egyptian_Hotel_name=Equinox+El+Nabaa+Resort&Egypt_City=Marsa%20Alam&hotel=205&offer=1

3- Flamenco Hotel – El Qusseir
http://www.flamenco.com.eg/quseir/diving.html

Eastern Desert of Egypt Field Conference Feb. 17-23, 2007 Informal Field Guide

The East African Orogen (EAO) marks one of earth's greatest collision zones, a global feature in space (about 6000 km long where it is preserved in Africa and Antarctica; Fig. 1) and in time (350 million years of evolution) (Stern, 1994). The EAO formed when fragments of East and West Gondwana collided, beginning ~630 Ma ago (Meert, 2003). The southern part of the EAO is also known as the Mozambique Belt and is thought to be where the most intense continent-continent collision occurred. The Mozambique Belt is thus dominated by deformed, metamorphosed, and anatectically reworked older crust.

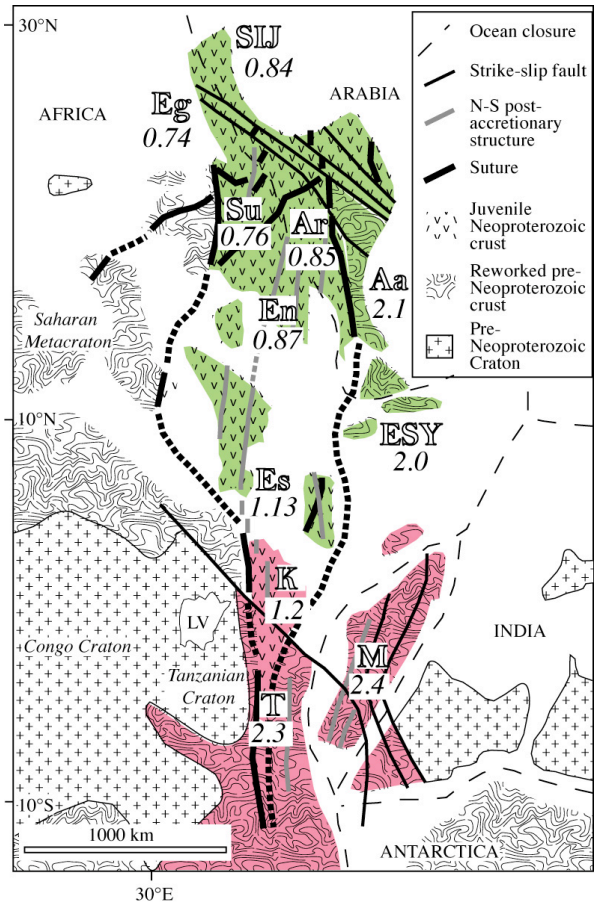

Figure 1: Simplified map of the East African Orogen with ocean basins closed. Abbreviations in large letters are regions where Nd model ages have been compiled (SIJ = Sinai-Israel-Jordan; Eg = Eastern Desert of Egypt, Su = NE Sudan; Ar = juvenile Arabia; Aa = Afif terrane Arabia; En = northern Ethiopia and Eritrea; Es = southern Ethiopia; ESY = eastern Ethiopia, Somalia, and Yemen; K = Kenya; M = Madagascar; T = Tanzania. Numbers beneath abbreviations are mean Nd model age, in Ga. Regions in pink appoximate the Mozambique Belt; areas in green approximate the Arabian-Nubian Shield. Modified after (Stern, 2002).

In contrast, the northern part of the EAO is mostly juvenile crust of the Arabian-Nubian Shield (ANS; Fig. 2 (Stern, 2002; Stoeser and Frost, 2006)). This assessment is based on the isotopic composition of igneous rocks (Fig. 1), which generally shows no hint of older crust. On the other hand, pre-Neoproterozoic crust has been identified in the Khida terrane in the SE Arabian Shield (Stoeser et al., 2001; Whitehouse et al., 2001) and older zircons are increasingly being recognized in igneous rocks where analyses of bulk-rocks yield juvenile isotopic compositions (HargroveIII et al., 2006b).

It now appears that the oldest Neoproterozoic rocks in the ANS are ~870 Ma, from the Asir terrane of Arabia and southern Red Sea Hills of Sudan (Kröner et al., 1991). It is important to understand how the ANS orogenic cycle began, and this is the region where it would best be studied. The evolution of the ANS takes place over 330 million years, from this time until about 540 Ma when the great peneplain is cut and great thicknesses of Cambro-Ordovician sandstones are deposited. It should be noted that the lower Paleozoic sandstones, which invariably overly the basement in Arabia, are almost totally missing in Egypt. These were mostly removed during Cretaceous uplift and erosion, so that the oldest sediments lying on the Egyptian basement are the Nubian sandstones of Cretaceous age.

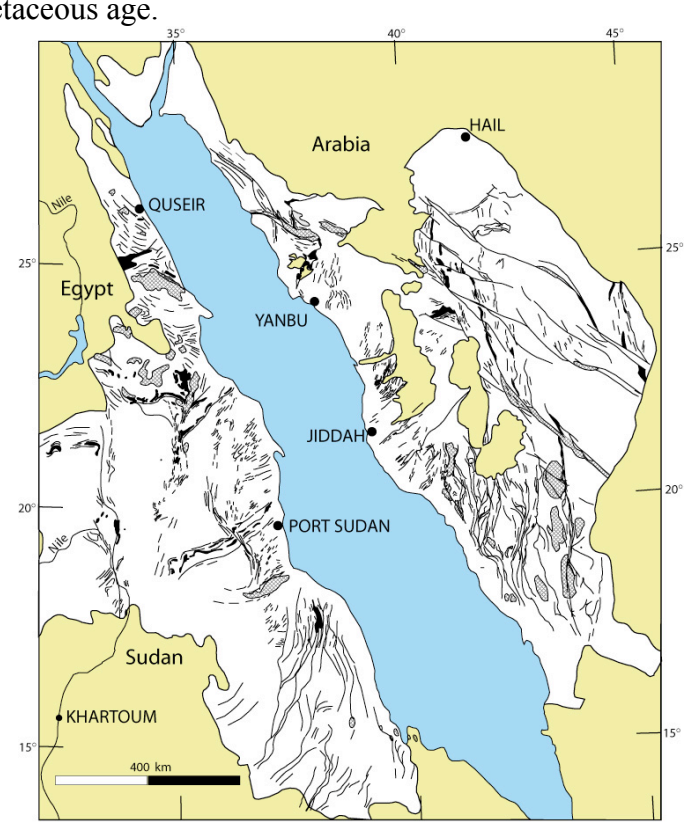

Figure 2: Simplified map of the Arabian-Nubian shield. Basement outcrops are white, Phanerozoic cover is shown in yellow. Structural trends are highlighted; ophiolitic rocks are shown in black and gneissic rocks shown in stipple. From (Johnson and Woldehaimanot, 2003).

The purpose of this field conference is to encourage collaborative research to better understand Neoproterozoic crust formation processes and mineralization in the

northern ANS. The hope is that we can stimulate efforts to correlate units across the Red Sea, between Egypt, Jordan, and northern Arabia; to carry out state-of-the art investigations into the age, composition, stratigraphy, and deformation history of the basement of this region; and to use this information to better understand how this crust formed, what this tells us about Neoproterozoic crustal evolution in general, and what controls basement-hosted mineralization. The status of basement correlation across the Red Sea between Arabia and Egypt is outline in a document at the end of this report (Potential Neoproterozoic Correlations between Al Wajh (Saudi Arabia) and Marsa 'Alam (Egypt) and Recommendations for Further Work, by Johnson and Kattan). This field conference is another step in that effort, and we focus here on a few places where important features of the basement can be studied.

Please note that we do not have time to visit the very interesting Neoproterozoic basement of Sinai. This basement is similar in many ways to the basement of the NE Desert, especially in the abundance of granitic rocks and the scarcity of ophiolite, BIF, diamictite, and other features characteristic of the Central Easterrn Desert. Like the basement of the SE Desert, the basement of Sinai is worthy of investigation but would require too much time to access during this short field conference.

A number of pdf reprints of articles has been posted on the web at
http://www.utdallas.edu/~dxt038000/Egypt%20Website/
Click on the NE Desert, CE Desert, SE Desert, and two other "click here" sites to access and download these. As of this writing, there are 111 articles posted.

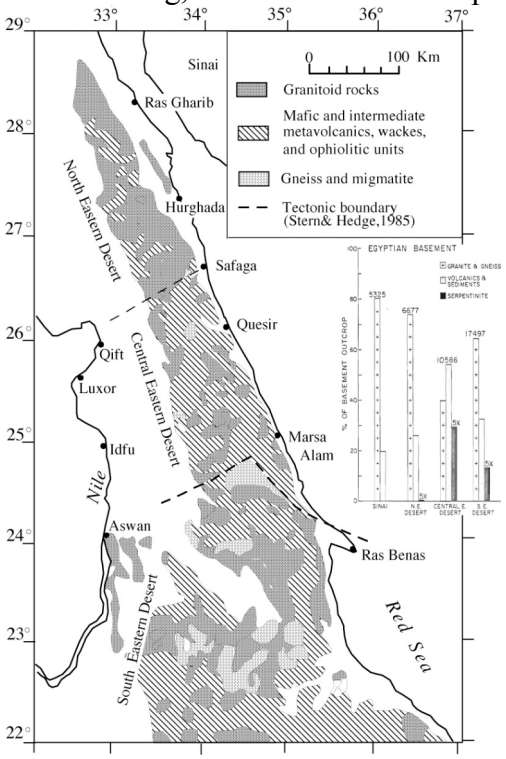

Figure 3: Simplified geologic map of the Neoproterozoic basement exposed Eastern Desert of Egypt. Map is modified from (Moussa et al., submitted). Inset shows relative abundances in the 4 major basement provinces of Eastern Egypt, from (Stern and Hedge, 1985)

We start with the Eastern Desert of Egypt, where ~100,000 km^2 of Neoproterozoic crust is exposed as a result of uplift related to the Oligocene and younger opening of the Red Sea (Fig. 3). In this field guide, the nature of interesting and important controversies is stressed. The hope is that highlighting controversy will stimulate research. Controversies are numbered in this field guide, in no particular order. A simplified stratigraphic column is shown in Fig. 4. This is based on regional relationships observed in the Central Eastern Desert and is certainly wrong in detail – for example at Wadi Kareim we will see the andesitic volcanics below the sediments which hosts the Banded Iron Formation (BIF) and the Atud diamictite (conglomerate in Fig. 4); we have not seen the diamictite lying on the ophiolite; and the Dokhan and Hammamat are approximately consanguinous. Nevertheless, this stratigraphic column does present the most important basement units and is useful as long as it is not taken literally.

The Egyptian ophiolites provide a useful reference point for understanding the formation of basement in the region. There is only one good age for Egyptian ophiolites, the 746±19 Ma age for the Ghadir ophiolite (Kröner et al., 1992) although ophiolites elsewhere yield Cryogenian ages as shown in Table 1.

Table 1. *A review of geological features that are indicative of an oceanic crust*

Area	Lithology	Age (Ma)	References
Wadi Ghadir, Egypt	Layered gabbros, sheeted dykes, pillow lavas, black shales	746 ± 19 (Pb–Pb)	El Akhal (1993); Kröner (1985); Kröner *et al.* (1992)
Qift-Quseir, Egypt	The Eastern Desert Ophiolitic Melange Group/Abu Ziran Supergroup: Dunites, peridotites, layered gabbros, sheeted dykes, pillow lavas and deep sea sediments (red pelites)	*c.* 800	Ries *et al.* (1983); Kröner (1985); El Gaby *et al.* (1984)
Onib and Gerf, Sudan	Ultramafic cumulates, interlayered gabbros, sheeted dykes and pillow basalt	*c.* 840–740, e.g. 808 ± 14 (Pb–Pb), 741 ± 21 (Pb–Pb)	Stern *et al.* (1990); Kröner *et al.* (1987)
Ophiolites throughout Saudi Arabia	Peridotites, gabbros, sheeted dykes, pillow lavas, chert, pelagic metasediments and marble	882 ± 12 (U–Pb) to 743 ± 24 (Sm–Nd)	Brown *et al.* (1989); Kemp *et al.* (1980); Claeson *et al.* (1984); Pallister *et al.* (1988)

Based on the 1972 geologic map of Egypt (El-Ramly, 1972), (Stern and Hedge, 1985) identified 3 distinct basement domains in the Eastern Desert; these are the North, Central, and South Eastern Deserts (Fig. 3), and are abbreviated NED, CED, and SED. This tripartite subdivision reflect the following: 1) there is a much higher concentration of granitic rocks in the NED and SED than in the CED; 2) ophiolites and serpentinites are absent from the NED; 3) gneisses are most abundant in the SED; and 4) the CED exposes by far the greatest concentration of rocks with strong oceanic affinities, such as ophiolites and BIF (ensimatic complex). The ~730 Ma Atud diamictite is also concentrated in the CED and SED and is missing from the NED, as is most gold mineralization. Najd deformation, which is very well-developed in Arabia, can be traced into the CED and perhaps the SED but not the NED (Sultan et al., 1988).

Diagnostic lithologies also occur in a sequence from earlier, primitive, to younger, enriched. The plutonic rocks can be subdivided into an calc-alkaline, orogenic, suite of older granodioritic rocks and a younger suite of A-type, postorogenic/anorogenic suite of younger granites, sometimes called the Pink Granites. As shown in Fig. 6, the time of transition between orogenic and postorogenic suites is ~600-615 Ma in Egypt, 608-615 Ma in Jordan, and 610-625 Ma in southern Israel (Beyth et al., 1994). The transitional period approximates the time of terminal collision along the EAO.

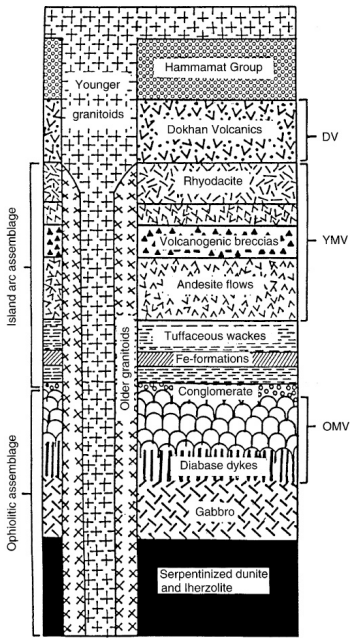

Figure 4: Simplified stratigraphic column for Neoproterozoic rocks of the Eastern Desert. OMV = older metavolcanics, YMV = younger metavolcanics, DV = Dokhan Volcanics. Figure is from (Mohamed et al., 2000).

These variations are summarized in Figure 5.

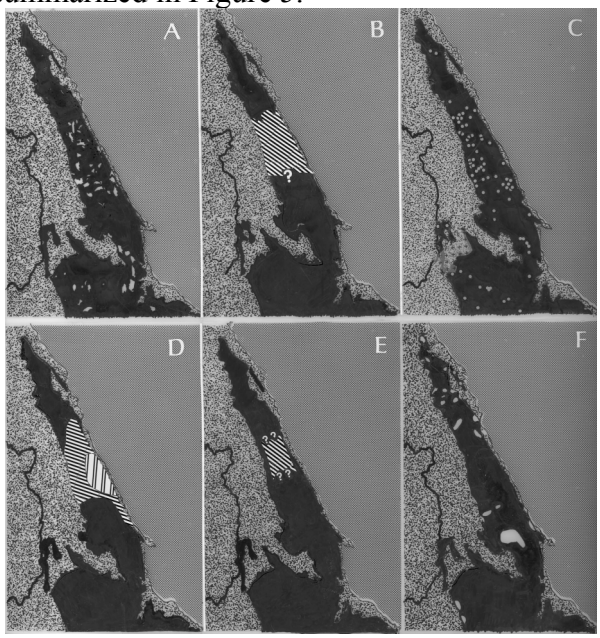

Figure 5: Distribution of diagnostic lithologies in the Eastern Desert, from (Stern, 1979). A) ultramafic rocks (mostly ophiolites); B) Geographic limits of older metavolcanics (mostly pilowed tholeiites); C) Gold deposits; D) Banded Fe Formation and jasper; E) Geographic limits of younger metavolcanics, mostly andesitic; F) Dokhan volcanics. Note that gold deposits are concentrated in the CED, with important implications for exploration in northern Arabia.

The abundance of granitic rocks in the NED invites comparison with the basement of the northernmost Arabian Shield, especially Jordan, where (Jarrar et al., 2003) note that ~90% of basement exposures in southern Jordan consist of intrusive rocks. The Jordanian granitic rocks are grouped into two major subdivisions: the Aqaba (600–640 Ma) and the Araba (560–600 Ma) complexes. Aqaba complex suites range in composition from gabbro to high silica granite (45–80% SiO_2) and follow a high-K calc-alkaline trend. This phase, which started with the emplacement of the Duheila Hornblendic Suite between 640 and 600 Ma, represents the main crust-forming stage in southwest Jordan.

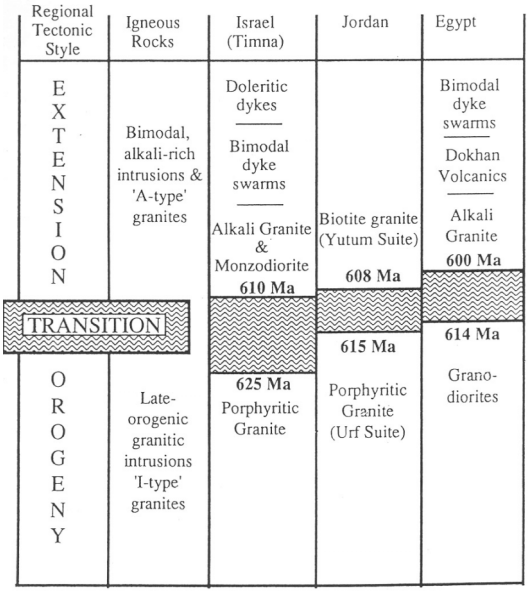

Figure 6: Timing of transition between older orogenic tectonics and magmatism and younger post-orogenic extension-related magmatism and tectonics in Israel, Jordan, and NE Egypt. Whether or not these relations are also found for the rocks of NW Arabia is not yet clear. From (Beyth et al., 1994).

It should be noted that most of the radiometric ages for Egyptian rocks are Rb-Sr whole rock determinations, which yield reasonably good ages for the Younger Granites, because these have high Rb/Sr. In contrast, this technique does not yield very precise or reliable ages for the older granitoids, so we have much more uncertainty about these ages of these rocks. Consequently, the age of the oldest Neoproterozoic igneous rocks in the Eastern Desert is controversial. Fortunately, the older granitoids are rich in zircons with low to moderate contents of U and Th and thus well-suited for U-Pb zircon dating, whereas the high U zircons in the Younger Granites often suffer a lot of radiation damage and thus give poor ages with this technique.

There is still a lot of uncertainty about how the plutonic rocks of the ED should be subdivided. A recent regional study in the Um Gheig province in the CED identifies five suites: Gabbro-diorite suite, Older granitoid, I-type younger granitoid, A-type younger granitoid, and Garnet-bearing granitoid suites. The first 2 suites are foliated whereas the last 3 are not (El-Sayed et al., 2002).

Other lithologies also manifest a change from orogenic to post-orogenic phases slightly before 600 Ma. Less-deformed (Hammamat) sediments and (Dokhan) volcanics and abundant dike swarms are common after this time, and much more deformed supracrustal sequences mostly being older than this. One exception to the general rule that the younger rocks are less deformed results from activity of Najd strike-slip faulting and shearing and from the presence of metamorphic core complexes (Blasband et al., 2000). Similar biases in radiometric dating exists, with good ages for the ~600 Ma Hammamat and Dokhan (Wilde and Youssef, 2000; Wilde and Youssef, 2002) and less reliable ages for older metavolcanic rocks of the arc and ophiolitic succcessions (Stern, 1981; Willis et al., 1988).

There are a number of vigorous controversies about the evolution of the Eastern Desert basement. **Controversy 1** is whether or not pre-Neoproterozoic crust, sometimes referred to as "fundamental basement" underlies Neoproterozoic crust. A lot of Egyptian geologists hold to this view (Botros, 2004; El-Gaby et al., 1988), but western geologists do not. There are points of agreement, specifically that the basement of especially the CED can be subdivided into "tier 1" gneisses and structurally overlying "tier 2" low grade successions (Bennett and Mosley, 1987; Greiling et al., 1994). This is equivalent to identifying infrastructure and suprastructure within the basement.

Lithologically and geochemically Tier 1 rock sequences are similar to those of Tier 2, namely oceanic lithosphere and island arcs. The gneisses are distinct from the low grade rocks only by their metamorphic grade and fabric. This deformational fabric has no age implication but is, apparently, an expression of the general increase in deformation intensity towards depth. Consequently, gneissic domains usually represent relatively low crustal levels and the surrounding low grade rocks can be taken as representing upper crustal rocks.

The Egyptian basement in the Central Eastern Desert was subdivided by (El-Gaby et al., 1984) into three major rock groups: Meatiq Group (oldest), Abu Ziran Group and Hammamat/Dokhan Group (youngest). They argued that the Meatiq Group represented pre-Neoproterozoic basement. The Abu Ziran Group comprises "geosynclinal association" formed of a lower ophiolite unit overlain by metasediments, volcanoclastics and locally intermediate volcanics having clear island arc characteristics. In contrast, most detailed studies since (Sturchio et al., 1983) made the original suggestion have concluded that the Meatiq Dome was an extensional core complex (Fritz et al., 2002; Loizenbauer et al., 2001; Neumayr and Khudeir, 1998). (Fritz et al., 2002) generated Ar/Ar ages for hornbende and muscovite from three large CED core complexes: Meatiq Sibai, and Hafafit (Fig. 7). They concluded that cooling accompanying exhumation was highly diachronous, with hornblende ages clustering around 580 Ma for Meatiq and Hafafit, and 623 and 606 Ma for Sibai. They argued that early-stage low velocity exhumation was triggered by magmatism beginning ~ 650 Ma in Sibai. Late stage exhumation was facilitated by combined effects of strike-slip and normal faulting, which continued until ~580 Ma. They argued that continuous magma generation weakened the crust, facilitating lateral extrusion tectonics, and that no major crustal thickening was required to form CED core complexes.

Isotopic compositions and ages of the major gneiss bodies in the Eastern Desert and Sinai do not support the inferences of underlying pre-Neoproterozoic crust (Stern, 2002) but there are tantalizing hints that pre-Neoproterozoic crust is in the vicinity. Such

evidence is found in the ancient cobbles of the Atud diamictite (Stern et al., 2006) and in the recognition of pre-Neoproterozoic zircons recovered from Neoproterozoic volcanics (Ali, unpublished data) and some granites (Sultan et al., 1990).

Controversy 2 concerns the interpretation that much of the crust of the Arabian-Nubian Shield formed by accretion of oceanic plateaus. This was originally proposed by (Stein and Goldstein, 1996) but never found much support from those of us who actually work in the ANS. This attractive but unfounded idea was recently reiterated in a Nature review by (Hawkesworth and Kemp, 2006), who drew attention to ".... the plume affinity of basaltic rocks associated with vast tracts of juvenile crust formed over short time periods, such as in the .... the Arabian-Nubian Shield." If there are plume-related igneous rocks in the Eastern Desert of Egypt, they are doing a good job of disguising themselves!

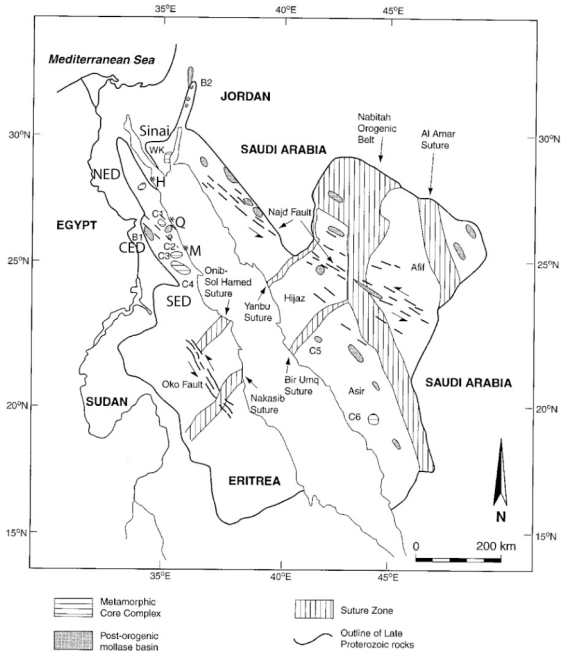

Fig. 7: Map showing the main Neoproterozoic features in the ANS, along with the location of ~600 Ma gneiss domes and associated sedimentary basins, modified after (Blasband et al., 2000). WK = Wadi Kid Complex; C1=Meatiq Dome; C2=El Sibai Dome; C3= Wadi Ghadir Complex; B1=Basin with Hammamat sediments; B2=Basin with Saramuj Conglomerate. H= Hurghada, Q= Quesir, M = Marsa Alum.

Controversy 3 concerns the age of the "Younger Metavolcanics", generally regarded to represent intra-oceanic arc material that makes up a very large part of CED crust (Figs. 4,5). The only published ages are Rb-Sr whole rock ages of 622±6 Ma (5 points) for Wadi El Mahdaf (~25°45'N, 33°39'E) and 632±28 Ma (10 points) pooled from outcrops along Wadi Arak (~25°46'N, 33°52'E) and Wadi Massar (~25°38'N, 33°47'E). These ages are much younger than the kinds of ~750 Ma ages obtained for the ophiolites. The YMV that UTD graduate student Kamal Ali is studying at Wadi Kareim and Wadi Dabbah yield zircon ages of ~740 Ma. These considerations suggest that the Rb-Sr ages are wrong because they are partially reset or there is an unrecognized unconformity or terrane boundary, or some combination of these. It is likely that samples of much younger "Atalla felsite" were included in the Arak-Massar isochron, as

suggested by the high MSWD obtained. This felsite is common in especially the northern part of the CED. The significance of this felsite is not yet well understood (Abdeen and Greiling, 2005; Essawy, 1974; Greiling et al., 1994), but it is worth further study. **Controversy 4** concerns whether or not the metamorphic equivalent of Atalla felsite comprises the quartzofeldspathic gneisses and mylonites of the Meatiq dome or whether these are shelf sediments. This controversy is easily resolvable with U-Pb dating of zircons, if shelf sediments there should be abundant pre-Neoproteozoic zircons, if felsite there should be few.

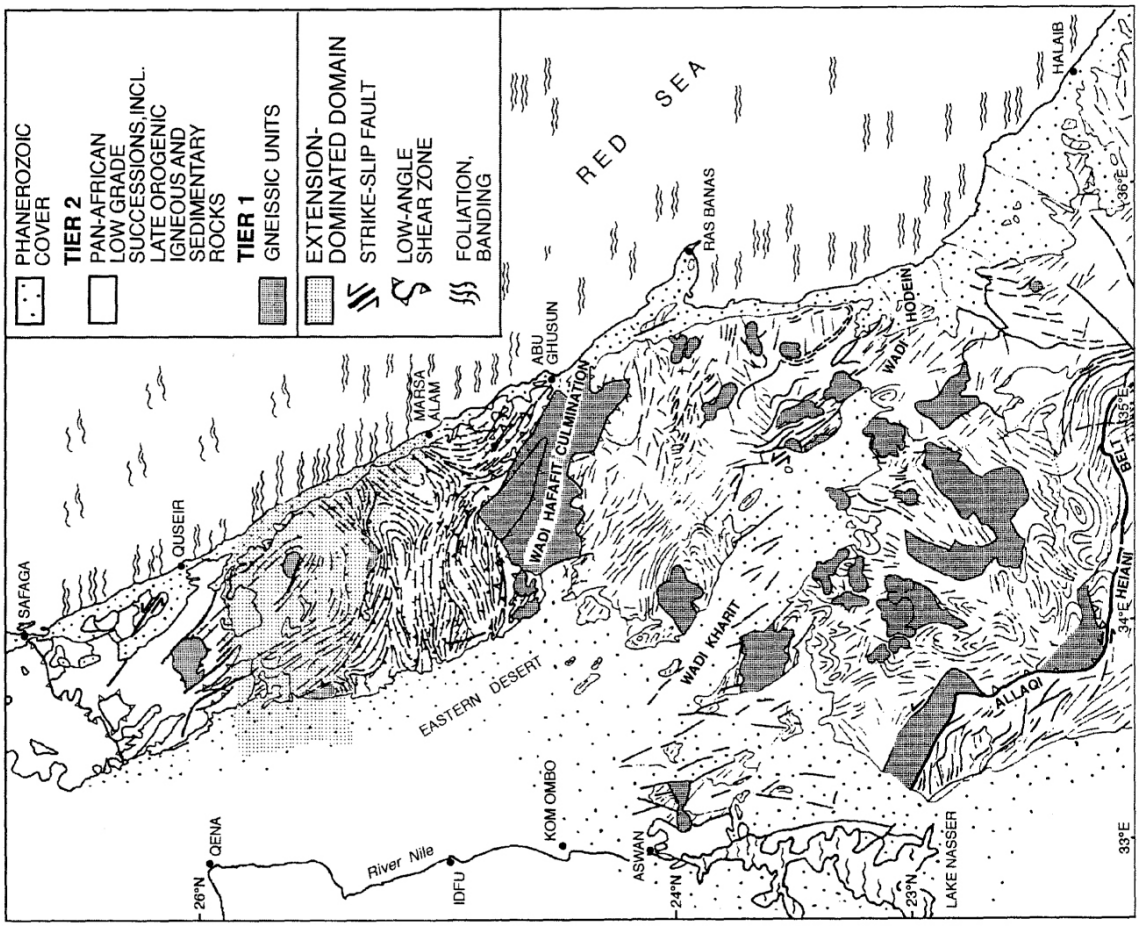

Figure 8 : Structural compilation map of the Neoproterozoic basement in the Eastern Desert of Egypt, from (Greiling et al., 1994). Most of the tier 1 gneissic units in the northern part of the map area form structural culminations, whereas a number of gneissic units in the south form fault-bounded slices or horsts, imbricated into tier 2 low grade successions. For the sake of clarity the tier 1 gneisses are shown without their internal structural grain, which is usually discontinuous across the margins and more complex than that of the surrounding tier 2.

Controversy 5 concerns what tectonic forces deformed the pre-600 Ma rocks of especially the Central Eastern Desert. Some workers interpret the deformation as due to arc accretion (Ries et al., 1983; Shackleton et al., 1980) whereas others infer that Najd strike-slip faulting was mostly responsible (Stern, 1985). The author of this guidebook

does not feel qualified to summarize the structural evolution of the ED, except to reiterate that subsequent studies have verified the regionally pervasive nature of remarkably uniform NW-SE lineations that (Stern, 1985) used to infer the presence of "Najd" deformation in especially the CED. It is still a mystery how this dominantly sinistral strike-slip deformation relates, if at all, to NW-SE directed extension in the NED at about the same time. Najd deformation is certainly closely related to the development of metamorphic core complexes in the CED (Fritz et al., 2002; Loizenbauer et al., 2001) and presumably similar structures exist in NW Arabia.

Controversy 6 concerns the tectonic setting in which <600 Ma igneous activity of especially the NE Desert occurred. Some argue that Dokhan volcanic activity is related to post-collision extension (Moghazi, 2003; Mohamed et al., 2000; Stern and Gottfried, 1986; Stern et al., 1984), whereas others infer a convergent margin or arc setting (Abdel-Rahman, 1996; Eliwa et al., 2006).

We will take advantage of good accommodations along the Red Sea to enjoy several day trips to look at and discuss some of these rocks. Unfortunately, we must neglect the rocks of the SE Desert for this trip, even though this region contains the best-preserved suture (Allaqi-Heiani suture; (Abdelsalam et al., 2003; Stern et al., 1990; Zoheir and Klemm, 2006 in press)). This suture can be traced eastwards into Arabia as the Yanbu Suture and contains the best-preserved ophiolite in the Eastern Desert (Gerf ophiolite; (Zimmer et al., 1995)).

Day One: Today we will leave Hurghada and drive south towards Quesir, where we will spend the next two nights. At Safaga we will take the asphalt road towards Qena and look at mostly granitic rocks, along with an excellent exposure of ~600 Ma Dokhan volcanics and feeder dikes. These are exposed along the road where it cuts through G. Nuqrah. The Nuqrah massif is the best-preserved Neoproterozoic caldera structure in the Eastern Desert, and it nicely shows the relations between the younger granite and Dokhan ignimbrite. The stratigraphy is very well-preserved and interesting, and where I studied it in 1981 (south of the asphalt road; Fig. 12) it consists of Dokhan andesites near the base, locally pillowed (was it a caldera lake or submarine caldera?), succeeded upwards by rhyolite ignimbrites. Some of the tuffs have well-developed beds of large silica-rich concretions, or geodes. These ignimbrites can be traced laterally into a rhyolite porphyry, representing the hypabyssal neck of the volcano. The rhyolite porphyry in turn grades westwards into a coarse-grained younger granite that appears to have been intruded into the caldera ring-faults.

The Gebel Nuqrah felsic rocks yield a Rb-Sr whole-rock age of 581±7 Ma (Stern and Hedge, 1985). Recent U-Pb zircon ages indicate the younger granites are ~600 Ma. The caldera complex is developed on older granodiorites of the immense and poorly-studied Qena-Safaga batholith. Representatives of the older granodiorites have been dated at Mons Claudianus at 666 Ma (single fraction U-Pb zircon model age) (Stern and Hedge, 1985) and at Um Taghir along the asphalt road at 653±3 Ma (SHRIMP ion probe age) (Moussa et al., submitted). These granodiorites are intruded by E-W andesitic dikes, which might be feeders for the Dokhan volcanics at G. Nuqrah. A 11-point Rb-Sr whole-rock age of 686±28 Ma for andesitic flows at G. Nuqrah and dikes of similar composition to the west (Stern and Hedge, 1985) is problematic, because this – in conjunction with the granodiorite ages - suggests that there is ~50 Ma between eruption of the andesitic

volcanics at the base and felsic volcanics at the top of the caldera complex, when in fact the volcanic succession is quite conformable. The relations between the ~650 Ma Qena-Safaga batholith, E-W mafic dikes, pre-caldera mafic volcanics, syn-caldera felsic volcanics, and younger granitic rocks may comprise **Controversy 7.**

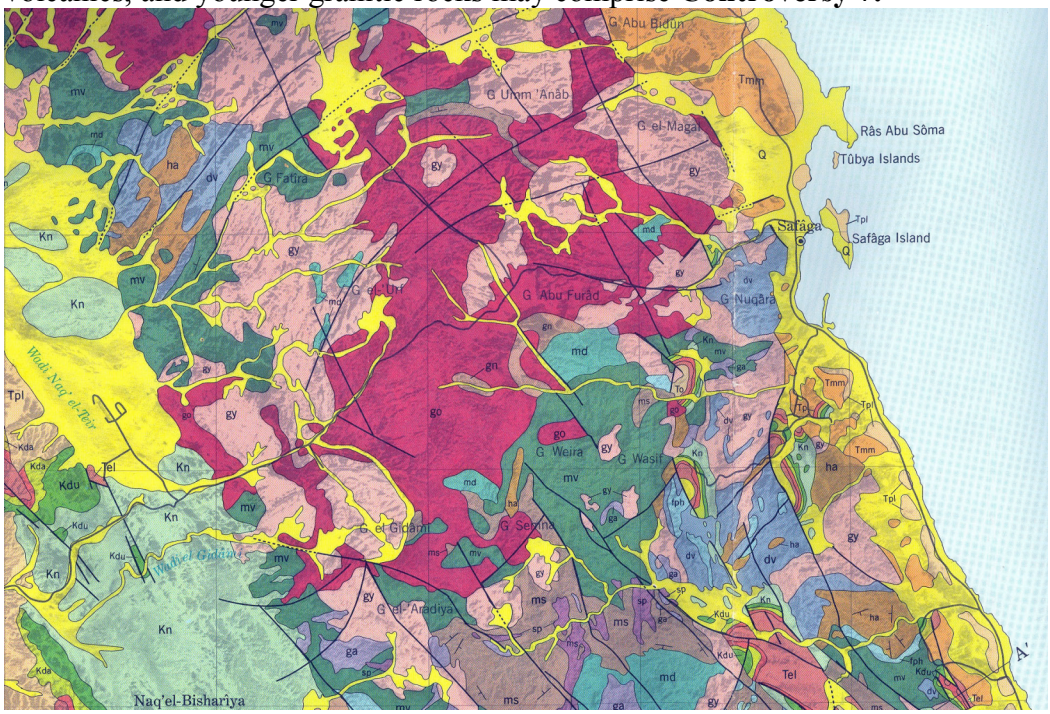

Fig. 9: Geology of the region west of Safaga, just north of the transition between the NE and Central Eastern Deserts. Region shown in Fig. 10 is G.Nuqrah and region to the west, just west of Safaga.

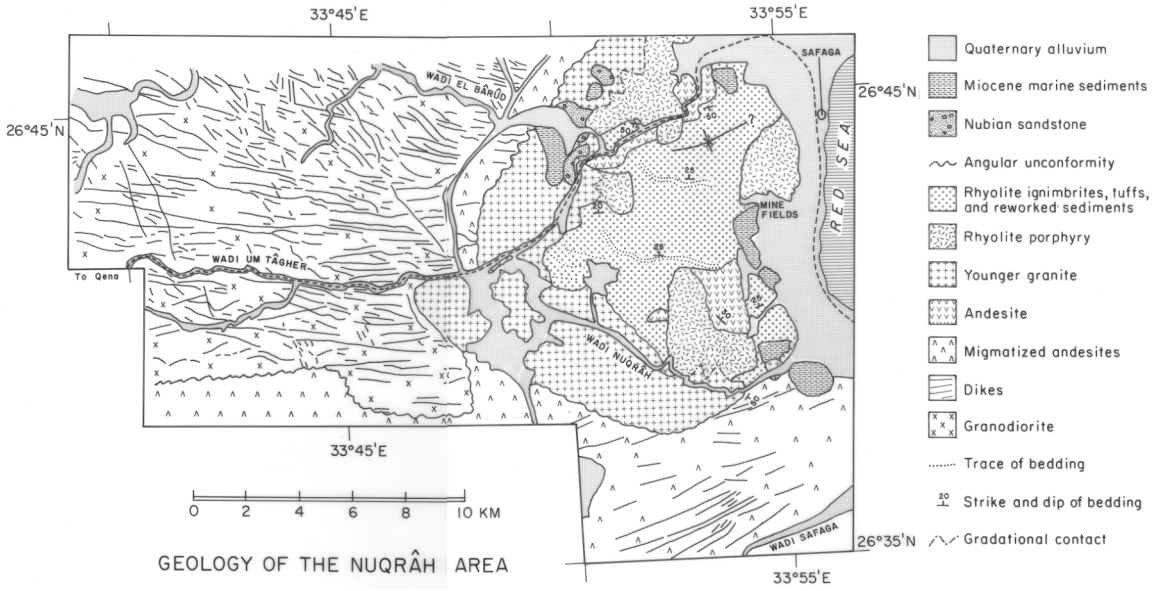

Fig. 10: Geology of Nuqrah caldera complex area, west of Safaga. Unpublished map of Stern (1981). Volcanic stratigraphy of Nuqrah caldera is shown in Fig. 11.

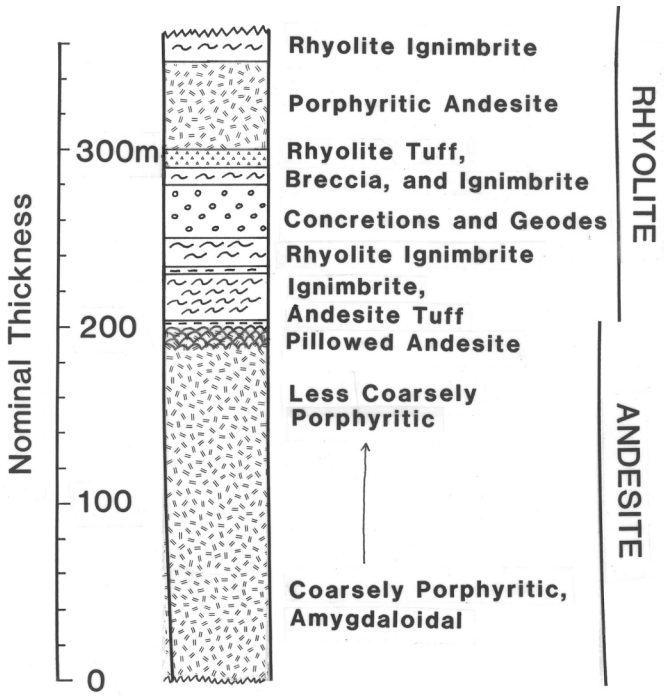

Fig. 11: Simplified stratigraphic column for the ~600 Ma Dokhan volcanics and related rocks of the Nuqrah caldera complex shown in Fig 10.

Day Two: Today we will travel along the Qena-Quesir road, traversing the lithologies and structures of the CED (Fig. 12). Just west of Quesir we will cross the Cenozoic Duwi- Hamadat half-graben, which preserves the Cretaceous and younger cover that lay

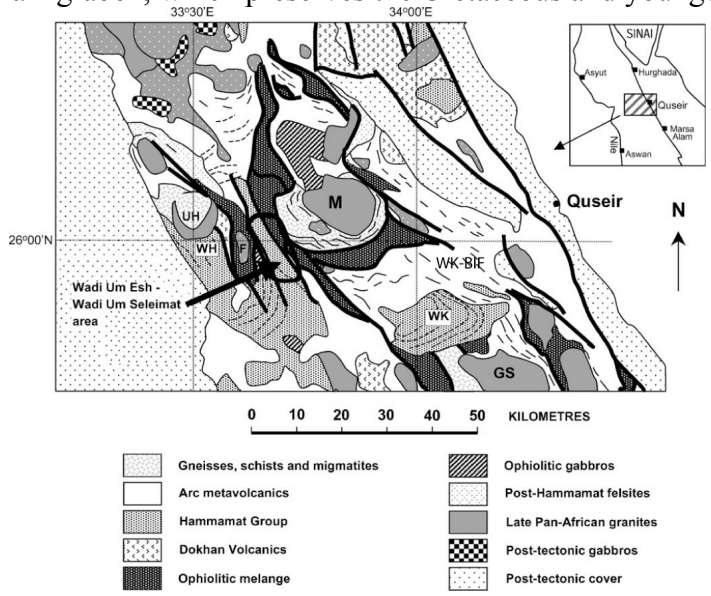

Fig. 12: Simplified geologic map for the northern part of the Central Eastern Desert, from (Fowler and Kalioubi, 2004). M=Meatiq Core Complex; F=Fawkhir Granite and ophiolite, UH=Um Had Granite; WH=Wadi Hammamat molasse deposits; WK=Wadi Kareim molasse deposits; GS=Gebel El-Sibai; WK-BIF= Wadi Kareim BIF. Bold lines are faults, short thin lines are foliation trends, broken lines are bedding trends. The Qena-Quesir road follows 26°N latitude approximately.

on top of the basement prior to Red Sea rifting and uplift (Khalil and McClay, 2002). This can be divided into a 300-700m thick section of Late Cretaceous to Middle Eocene pre-rift strata. The lower part is the ~130m thick massive, thick-bedded, siliciclastic Nubian Formation. This is overlain by 220-370m thick sequence of interbedded shales, sandstones, and limestones of the Quseir, Duwi, Dakhla, and Esna Formations. The uppermost pre-rift strata consists of 130-200m of thick-bedded limestones and cherty limestones of the Lower- to Middle Thebes Formation. Although not seen here, the Late Oligocene to Recent syn-rift strata unconformably overlie the Thebes Formation and vary in thickness from <100m onshore to as much as 5km offshore. The lowermost synrift strata are dominantly coarse-grained clastics (Nakheil and Range Formations). Overlying these clastics are reef limestones, clastics and evaporites of the Um Mahara, Sayateen, and Abu Dabbab Formations. Late Miocene carbonates and reefs aand Pliocene to Recent syn-rift clastics overlie the evaporites in the coastal outcrops. The SE extension of the Duwi half-graben in Arabia is probably the Azlam graben (Figure 13). This simple extrapolation is complicated by **Controversy 8**, because the Duwi half graben is tilted NE whereas the Azlam graben is tilted SW.

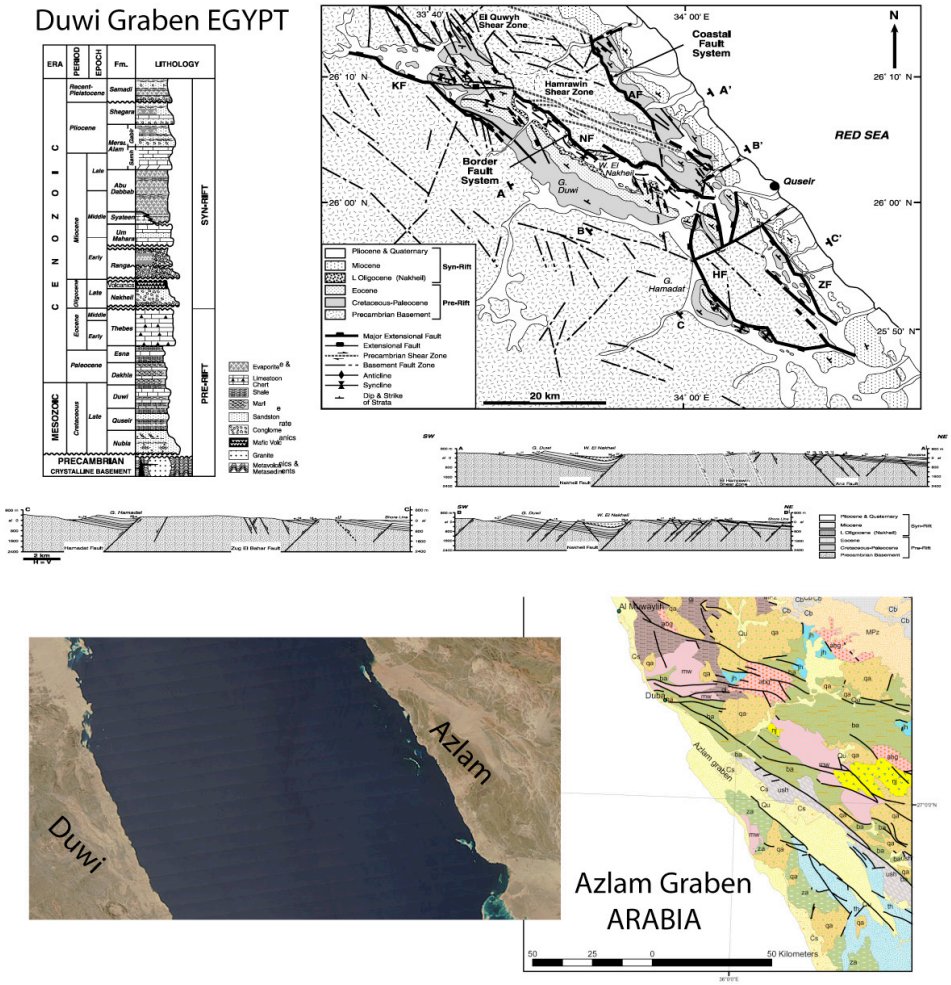

Fig. 13: Possibly correlative Cenozoic rift structures in Arabia and Egypt

One of the most important points of the Qena-Quesir transect is the Meatiq dome, which has been interpreted as a uplift that exposed "fundamental basement" or shelf sediments or as a metamorphic core complex associated with Najd strike-slip tectonics (**Controversy 9**).

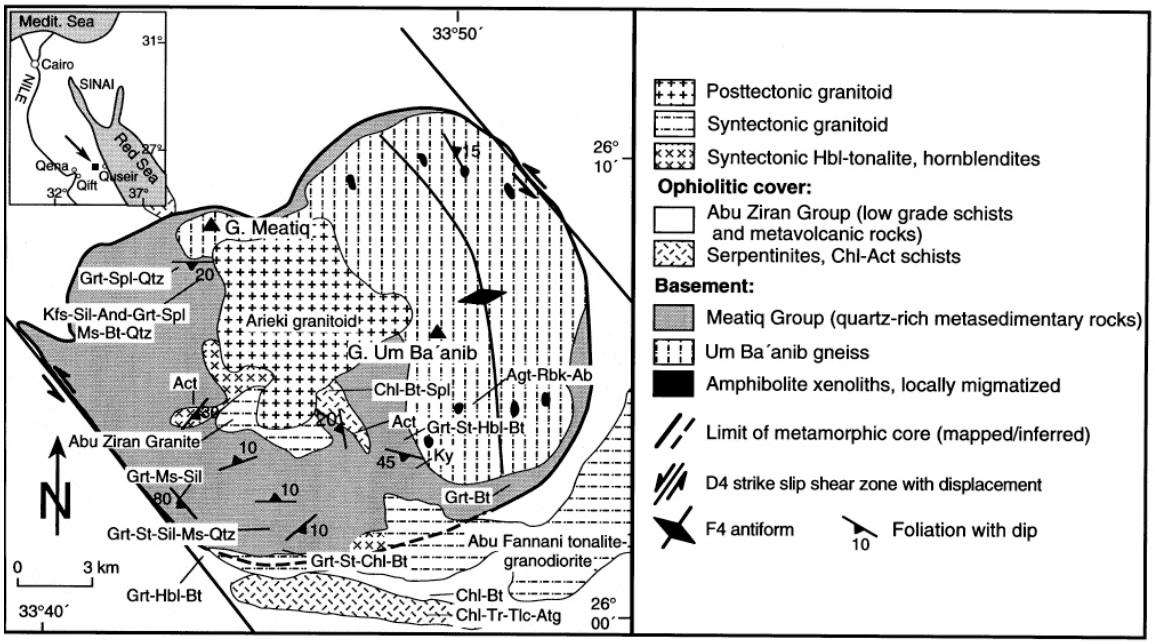

Fig. 14: Simplified geologic map of the Meatiq dome and environs. From (Neumayr and Khudeir, 1998). Table below is also from this source.

Table 1. Generalized geological history of the Meatiq basement dome and its ophiolitic mélange cover sequence.

Age (Ma)	Cover sequence	Metamorphism	Age (Ma)	Basement	Metamorphism
			579 ± 6[6]	Intrusion of postkinematic granitoids (Arieki tonalite); F5 folds coeval activation of NW-striking strike-slip shear zones and S- and N-directed low-angle normal faulting during uplift of the gneiss dome	
			585 ± 14[4]		
			595.9 ± 0.5[5]		
			588.2 ± 0.3[5]		
614 to 588	normal faulting, megascale strike-slip shear zones; in the external parts of the orogen (W of the Meatiq basement) development of fold and thrust belt	(lower?) greenschist facies	613 ± 5[3]	D4 mainly extensional crenulation cleavage (ECC) in metasedimentary rocks, chlorite growth in extension fractures in garnet; F4 Um Ba'anib antiform	
			626 ± 2[3]	intrusion of syntectonic granitoids	M3 greenschist facies
			614 ± 8[4]		
			>616	D3 planar (S3) foliation in the metasedimentary rocks, non coaxial fabrics including stretching of Grt (L3), initiation of megascale strike-slip faults	
? to 614	obduction of the ophiolitic mélange onto the basement, thrusting		>626	D2 ductile open to isoclinal and tight folds outlined by internal ilmenite trails in garnet; high T gneiss fabric in the Um Ba'anib gneiss	M2 upper amphibolite facies (610–690 °C, 6–8 kbar)
			780[2]	Intrusion of the Um Ba'anib granitoid	
880–690[1]	formation of oceanic crust		>780[2]	D1 migmatization of amphibolites, which are subsequently included in the Um Ba'anib gneiss; melt enhanced extensional fabrics	M1 migmatization (750–800 °C)

Structural evolution modified after Habib *et al.* (1985), Fritz *et al.* (1996) and this study. Metamorphic evolution this study. [1] Stern (1994) and references therein; [2] U. Klötzli (pers. com., 1996), Pb single zircon evaporation age; [3] Sturchio *et al.* (1983b), Rb/Sr isochron age; [4] Stern & Hedge (1985), conventional U/Pb age on zircons; [5] Fritz *et al.* (1996), $^{40}Ar/^{39}Ar$ on muscovite; [6] reported in Sturchio *et al.* (1983a), Rb/Sr model age.

Abundant serpentinites are exposed along the Qena-Quesir road. The most distinctive are linear zones of extremely altered serpentinites. This alteration is concentrated along thrusts and shear zones with the development of a range of talc, talc-carbonate and reddish brown quartz-carbonate rock (listwaenite). The most characteristic feature of listwaenite is its relative resistance against weathering, if compared with the

surrounding rocks; accordingly, listwaenite ridges define much of the topography of the CED. Listwaenites in the CED are sometimes referred to as "Barrimaya Rock" or "talc-carbonate" (El-Sharkawy, 2000). These ultramafics are almost certainly dismembered fragments of ophiolites. **Controversy 10** concerns the origin of the carbonate solutions which so pervasively altered the ultramafics and other pre-600 Ma assemblages, was this derived from sedimentary carbonates or mantle? There are not many sedimentary carbonates in the Eastern Desert. Intrusive carbonate bodies in the Eastern Desert of Egypt and Sudan were studied by (Stern and Gwinn, 1990), especially their C, O, and Sr isotopic compositions (Fig. 15). The isotopic data indicate three distinct reservoirs for these intrusive carbonates: (1) sedimentary carbonates, with moderately high $^{87}Sr/^{86}Sr$ and heavy C and O; (2) depleted mantle, with low $^{87}Sr/^{86}Sr$ and light C and O; and (3) enriched mantle or lower crust, with high $^{87}Sr/^{86}Sr$ and light C and O. Isotopic data indicate that the intrusive carbonates of the North Eastern Desert were derived from reservoir (2), and a sample from the interior of Sudan was derived from reservoir (3). The origin of the remaining intrusive carbonates of the Central Eastern Desert and Sudan is best explained as mixing between remobilized sedimentary carbonates and mantle fluids, i.e. reservoirs (1) and (2). The source of the sedimentary carbonates may have been carbonate bank sediments deposited during Neoproteozoic rifting and evolution of a passive continental margin on the north flank of the South Eastern Desert, now structurally buried under the Central Eastern Desert mélange. To date the careful work needed to see if a similar explanation fits the ophiolitic listwaenites and talc-carbonate rocks and when this alteration occurred.

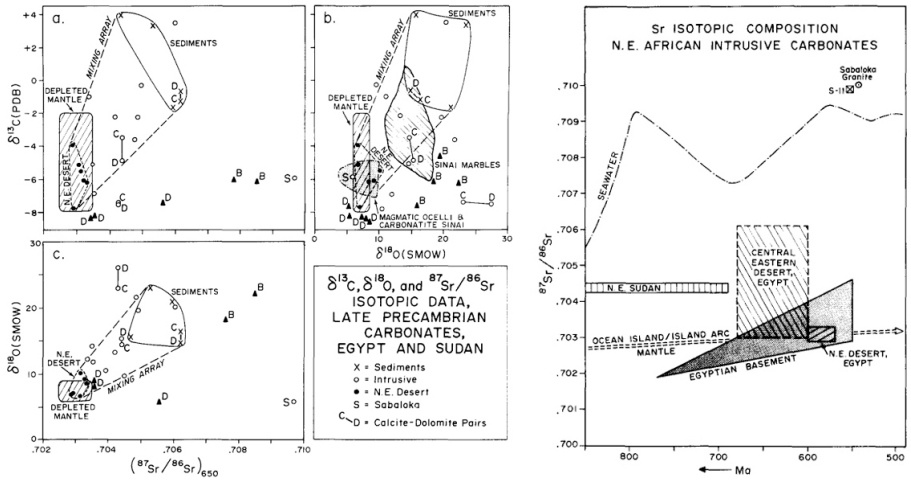

Fig. 15: Left: Plots of O, C and Sr isotope data for northeast African carbonates. (a) $\delta^{13}C$ vs. $^{87}Sr/^{86}Sr$ at 650 Ma, with fields for North Eastern Desert intrusive carbonates, sediments, and bulk mixing array. Data for Sinai carbonates are shown as filled triangles, marked 'D' (dolomite) or 'B' (breunnerite). (b) $\delta^{13}C$ vs. $\delta^{18}O$ for the same samples. The fields occupied by magmatic ocelli and carbonatite from Sinai and Sinai marbles of sedimentary origin are also shown for reference. (c) $\delta^{18}O$ vs. $^{87}Sr/^{86}Sr$ at 650 Ma. Right: Isotopic evolution of Sr in Neoproterozoic intrusive carbonates from northeast Africa. The ages of emplacement for the intrusive carbonates are estimated from the age of the surrounding basement units. Field of initial $^{87}Sr/^{86}Sr$ for the Egyptian

basementis also shown; this field represents an upper limit for the isotopic composition of Sr in the depleted mantle beneath northeast Africa at that time. Isotopic composition of Neoproterozoic seawater is also shown. Note that the fields for the Central Eastern Desert and northeast Sudan intrusive carbonates are displaced from the field for the Egyptian basement towards Neoproterozoic seawater. Note also that the close correspondence of initial $^{87}Sr/^{86}Sr$ for the Sabaloka granite and sample S l l suggest that both may originate in the lower crust.

Controversies 1 and 12 concerns the age and tectonic setting of ophiolites of the Eastern Desert. Ophiolites were first recognized in Egypt almost 50 years ago (Rittmann, 1958) but modern studies began with the work of (Bakor et al., 1976) in Arabia 30 years ago. Ophiolitic ultramafics of Neoproterozoic age are common in the CED and SED where they occur as highly altered serpentinites and talc-carbonate (listwaenite; Johnson et al., 2004) rocks enclosing rare relicts of fresher peridotite. Modern studies of Egyptian ophiolites began with studies of the Wadi Ghadir ophiolite (El-Sharkawy and El-Bayoumi, 1979). Since then, the serpentinites of Egypt have generally been interpreted as parts of tectonically emplaced oceanic lithosphere.

A good summary of ANS ophiolites can be found in (Stern et al., 2004) and good detail on Arabian ophiolites is provided by (Johnson et al., 2004).

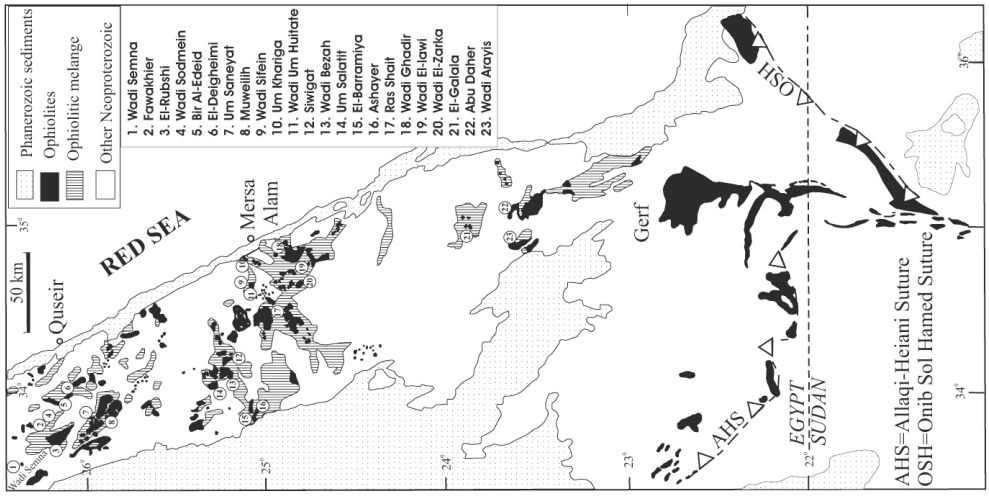

Fig. 16: Distribution of ophiolites and ophiolitic melange in the CED and SED, after (Azer and Stern, 2007 in press). Note that north is to the left.

Ophiolites of the northern ANS are generally interpreted to have been generated in supra-subduction zone (SSZ) tectonic settings (Bakor et al., 1976; Nassief et al., 1984; Pallister et al., 1988; Stern et al., 2004); similar interpretations hold for Egyptian ophiolites ((Ahmed et al., 2001; Azer and Khalil, 2005; El-Sayed et al., 1999; Farahat et al., 2004; Khudeir and Asran, 1992). Seafloor spreading necessary to form supra-subduction zone ophiolites occurs in fore-arcs during the "Infant Arc" stage of subduction initiation or in back-arc basins (Pearce, 2003). Most researchers infer a back-arc basin setting for Egyptian ophiolites (Ahmed et al., 2001; El-Sayed et al., 1999; Farahat et al., 2004); a fore-arc setting is rarely considered, partly because the hypothesis of fore-arc spreading during subduction initiation is relatively new (Stern, 2004).

Serpentinized ultramafics are very common in the CED, and are generally easier to recognized than are associated gabbros and metavolcanics because the serpentinites are buff-colored, resistant, and display distinctive cavernous weathering that makes them easy to identify from the window of a speeding car, whereas the latter develop thick desert varnish so that a fresh surface must be inspected. Stern et al. (2004) recognized that ANS ophiolitic ultramafics are mostly harzburgitic, containing magnesian olivines and spinels (Cr# = molar Cr/(Cr+Al) mostly > 0.60), comparable to spinels from modern fore-arcs, and distinctly higher than spinels from mid-ocean ridge and back-arc basin peridotites. This also seems to be true for Egyptian serpentinites (Azer and Stern, 2007 in press), as shown in Fig. 17.

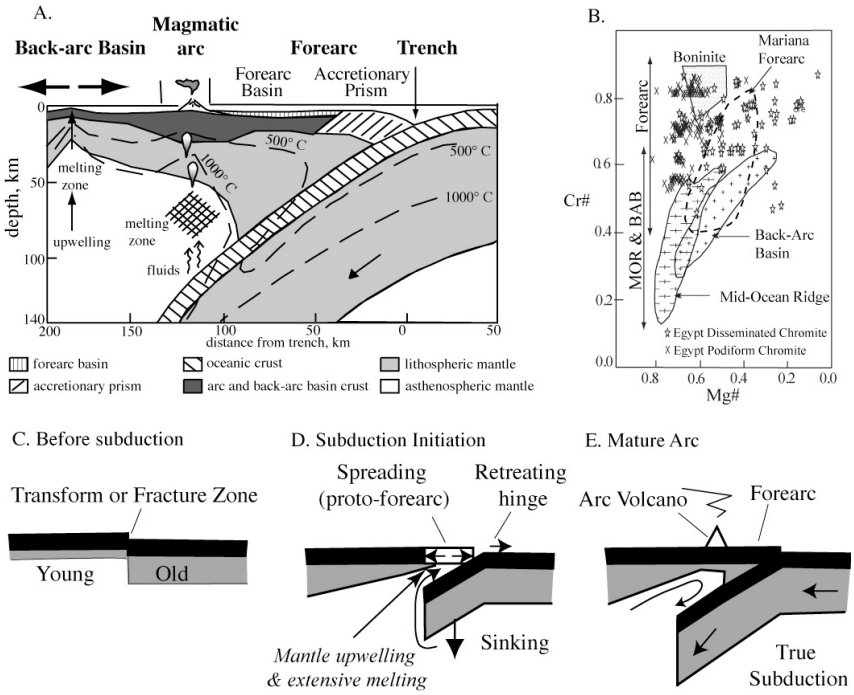

Fig. 17: Cartoons showing the tectonic setting of CED serpentinites based on spinel compositions in peridotites, modified after (Azer and Stern, 2007 in press). A) Cross section through a mature convergent margin, showing isotherms (dashed) and zone of melting beneath the arc and back-arc. Note complete absence of melting beneath the forearc of a mature convergent margin. B) Plot of Egyptian spinel Cr# = molar Cr/(molar Cr + Al) vs. Mg# =molar Mg/(molar Fe + molar Mg). Note that most Egyptian chromites have the high Cr# typical of forearc peridotite spinels. C-D-E: Cartoons from (Stern, 2004) showing formation of a subduction zone, from collapse of a transform margin (C) to lithospheric subsidence associated with asthenospheric upwelling and extensive melting (D), leading to the formation of very depleted boninites and forearc peridotites, ultimately leading to the formation of a mature convergent margin (E and A). Spinel compositions of Egyptian peridotites are consistent with formation in (D).

One of the best preserved ophiolites in the Eastern Desert outcrops around Bir Fawkhir or Bir El Sid (Fig. 18). This ophiolite is traversed by the Qena-Quesir asphalt

road, along which an westward-tilted succession of serpentinites, gabbro, sheeted dikes, and pillowed tholeiites has been thrust (Najd-related transpression?) over Dokhan Volcanics and Hammamat sediments and intruded by a younger granite. This is the type locality (Wadi El Hammamat), and here the Dokhan Volcanic Series has been thrust over the Hammamat Group.

This is also the location of the El-Sid gold mine. Gold deposits at El Sid are confined to hydrothermal quartz veins which contain pyrite, arsenopyrite, sphalerite and galena (El-Bouseily et al., 1985). These veins occur at the contact between the granite and serpentinite and extend into the serpentinite through a thick zone of graphite schist. Gold occurs either as free gold in quartz gangue or dissolved in the sulfide minerals. According to (Botros, 2004), the El-Sid gold deposit is a good example of vein-type mineralization hosted in sheared ophiolitic ultramafic rocks.

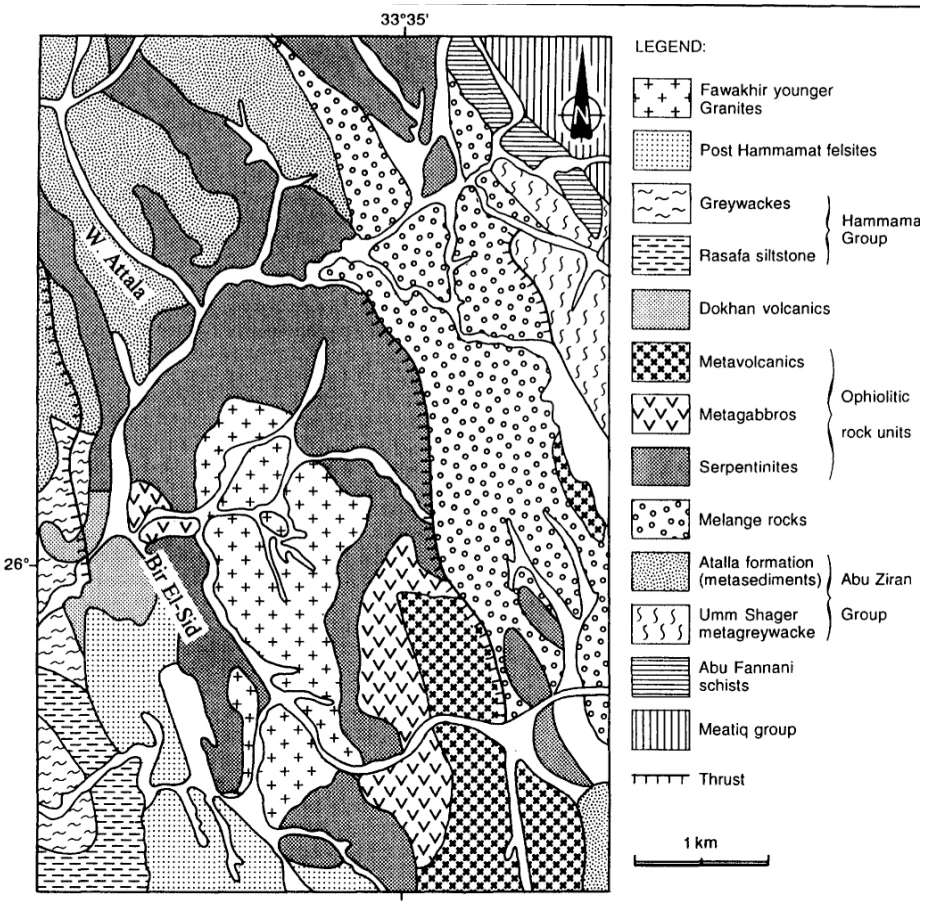

Fig. 18: Geologic map of the Fawkhir ophiolite, from (El-Sayed et al., 1999). See Fig. 12 for location.

According to (El-Sayed et al., 1999), the Fawkhir ophiolite contains igneous rocks that range from arc-type lavas, plume-type MORB, and boninitic rocks (Fig. 19). They inferred from this that the ophiolite formed in a back-arc basin. In contrast, (Azer and Stern, 2007 in press) boninitic rocks are diagnostic of forearc settings. The controversy about what tectonic setting the ophiolites formed in is important because forearc

ophiolites mark episodes when new subduction zones form (Stern, 2004), episodes that are associated with major plate reorganizations. In contrast, back-arc basins can form at any time in the evolution of a convergent plate margin.

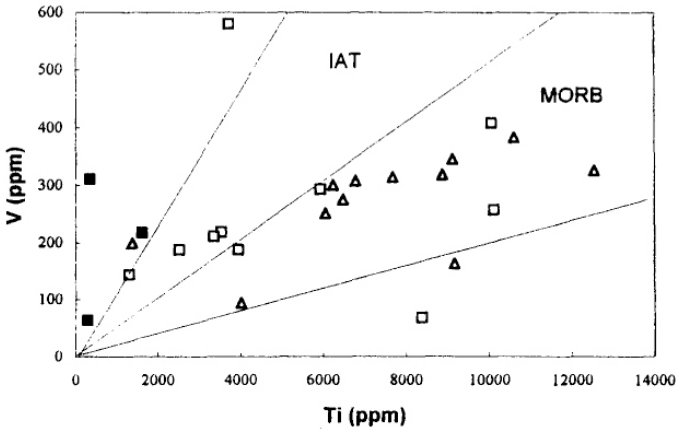

Fig. 19: Ti-V discrimination diagram for metagabbros (open squares), boninitic metagabbros (filled squares), and metavolcanics (open triangles) (El-Sayed et al., 1999)

The age of the Fawkhir ophiolite is unknown. As noted above, only one Pb-Pb age has been reported for Egyptian ophiolites, that of Wadi Ghadir, and especially the Fawkhir ophiolite (and related pillow basalts at the Arak-Zeidun intersection due south of Fawkir) may be significantly younger than ~750 Ma). At Arak-Zeidun there are extremely well-preserved pillowed tholeiites (Fig. 20 left) overlain by wackes and spectacular olistostrome deposits, some of which contain cobbles of pink, younger granite (Fig. 20 right)! This cobble is indistinguishable from ~600 Ma younger granites elsewhere in the Eastern Desert, implying that the olistostrome on top of this ophiolite is younger than ~600 Ma.

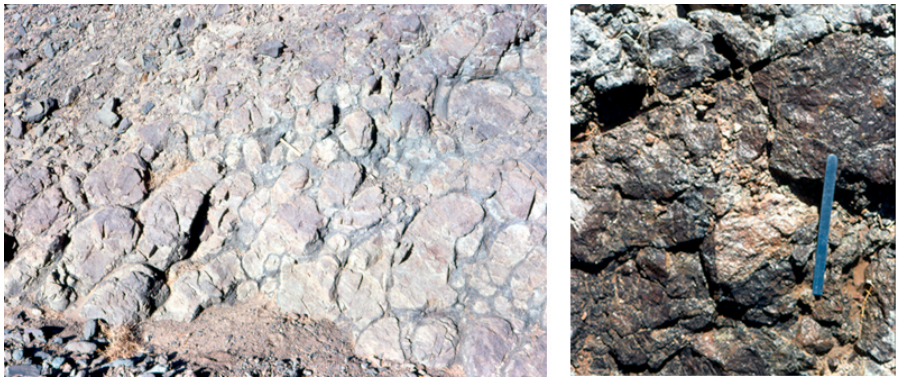

Fig. 20: (left) Ophiolitic pillowed tholeiitic basalts near the junction of wadis Arak and Zeidun, this is the southern extension of the Fawkhir ophiolite. Note rock hammer for scale. (Right) clast of pink granite in olistostromal sediments above pillowed basalts in Wadi Zeidun.

Controversy 12 concerns the significance of inherited zircons in ophiolites of the ANS. This has only been observed for the Thurwah ophiolite in Arabia north of Jeddah, but

experience there has important implications for zircon dating of Egyptian ophiolites. (Pallister et al., 1988) dated gabbro of the Tharwah ophiolite. A single coarse-grained zircon fraction yielded a nearly concordant U-Pb model age of 870 ± 11 Ma. Two other fractions were highly discordant and yielded model ages of ca. 1250 Ma. They attributed the older ages to assimilation of zircon from older basement material, but Late Mesoproterozoic crust is unknown from the ANS. This age is especially important because it is the oldest for any ANS ophiolite. (HargroveIII et al., 2006a) used the SHRIMP-RG in an effort to resolve the controversy, but were only partly successful (Fig. 21). Samples of moderately altered, coarse-grained, layered meta-leucogabbro collected only a few hundred meters from the locality sampled by Pallister and others (1988b) yielded nine zircon grains which form two arrays corresponding to the two samples, the horizontal trends of which suggest lead loss. The most concordant of the zircons in the older array yields a concordia age of ca. 1130 Ma, which approximates the age of inheritance. The younger array can be resolved into two points that are nearly identical and yield a concordia age of 777± 17 Ma (MSWD = 0.68) and two younger points that appear to have experienced lead loss. This two-point concordia age is weak, but there is no support for an age of 870 Ma obtained by Pallister and others (1988) for the Tharwah ophiolite. Clearly an important opportunity in ED studies is to better establish the ages of the ophiolites and to assess the significance of zircon inheritance in these bodies. How do ancient zircons find their way into regions where seafloor spreading occurs? In particular, how do inherited zircons from a time for which no crust is known anywhere in or near the ANS??

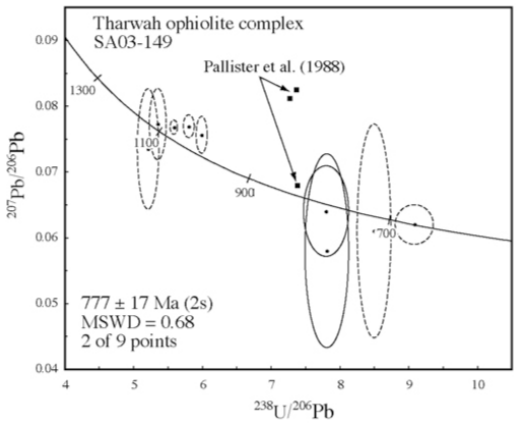

Fig. 21: Tera-Wasserburg concordia diagram for sample SA03-149 of layered gabbro from the Tharwah ophiolite complex, from (HargroveIII et al., 2006a). Data points are shown with 2σ error ellipses; dashed ellipses were excluded from age calculations. Data for conventional multi-grain analyses of Pallister et al. (1988) are also shown.

Day Three: Today we will travel west from Quesir and turn south to follow the western side of the Duwi-Hamadat graben towards the metavolcanic-diamictite-BIF exposures of Wadi Kareim (figs. 22, 23). UTD and NMA are collaborating to help UTD graduate students Sumit Mukherjee study the BIF here and UTD graduate student Kamal Ali to study the metavolcanics and Atud diamictite; the SGS is collaborating with these students to study similar units in Arabia (Ghawjah volcanics, Nuwaybah diamictite (Zaam Group), and Sawawin BIF). We will visit Wadi Kareim first and if time and

interest permits, continue

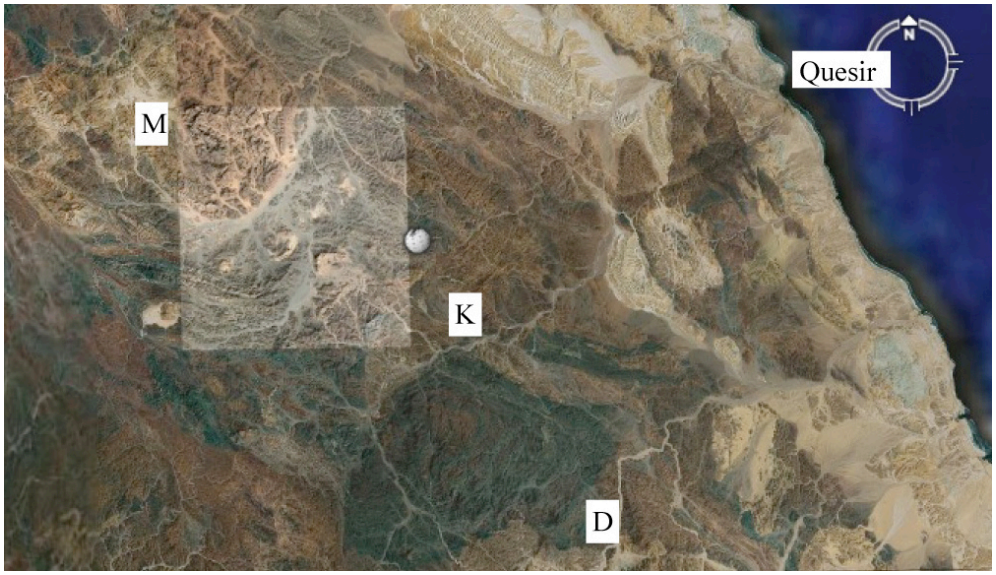

Fig. 22: Location of Wadi Kareim (K) and El Dabbagh (D) study areas. Location of Meatiq dome (M) is also shown. Dark green area between Kareim and Dabbagh is a Hammamat basin. From Google Earth.

to Wadi Dabbagh. Exposures north of Wadi Kareim show a continuous section from metavolcanics (YMV according to the classification of Stern 1981) overlain by wackes, Atud diamictite, and BIF (Fig. 24). This is the only place known in the ANS where the diamictite and BIF are found together (Figure). At Wadi Dabbagh the BIF is also associated with volcanics but there is no evidence of the diamictite (Fig. 24).

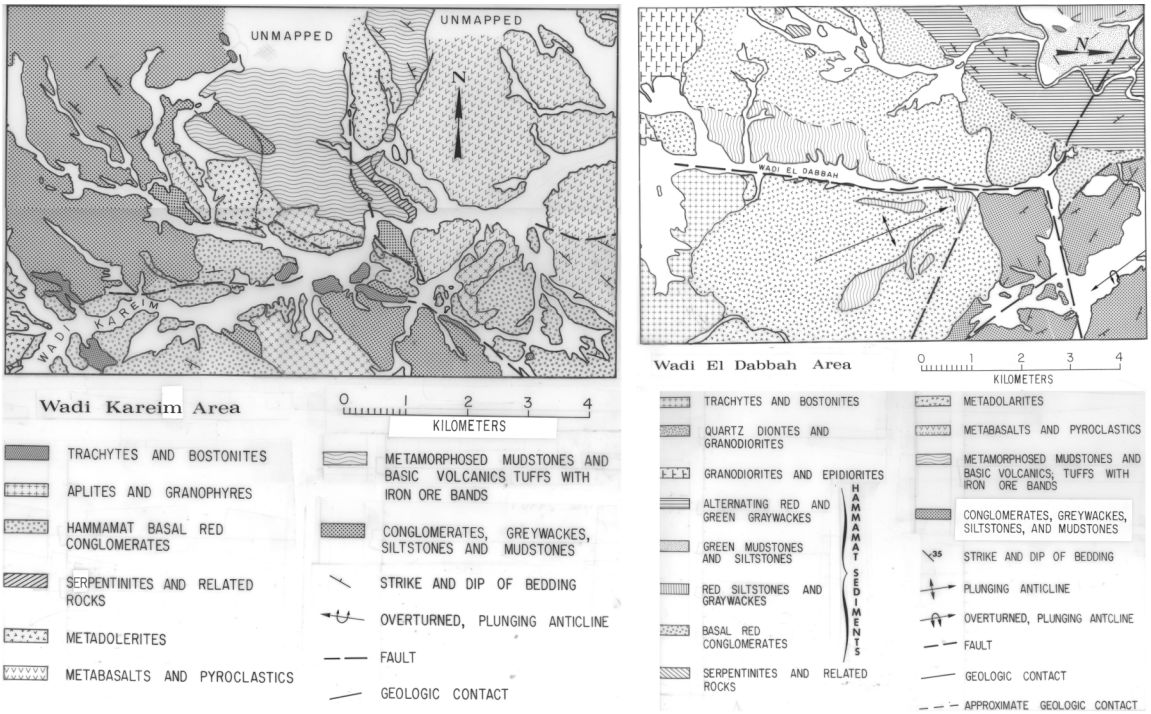

Figure 23: Geologic map of Wadi Kareim area (left) and Wadi El Dabbagh area (right; note north arrow (Stern and Dixon, unpublished)

The volcanics are low- to medium-K and often quite primitive (Fig. 25). Most show REE patterns that are slightly LREE-depleted to slightly LREE-enriched (Fig. 26). On extended trace-element diagrams they show the characteristic spikes in fluid-mobile elements (Sr, Pb) and depletions in Nb, similar to what might be expected for a juvenile (intra-oceanic) arc/back-arc basin system (Fig. 26). The Dabbagh YMV are generally more depleted than the Kareim YMV. The associated sediments indicate submarine depositional environments. There is certainly no geochemical evidence that these lavas erupted in association with a mantle plume.

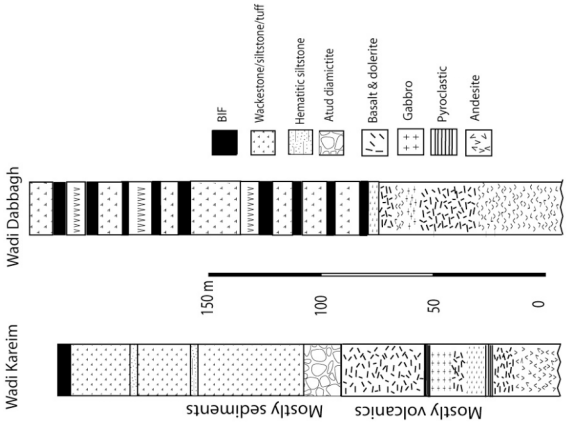

Figure 24: Simplified stratigraphy for YMV, BIF, and Atud diamictite at Wadi Kareim and Wadi Dabbagh (Ali, work in progress)

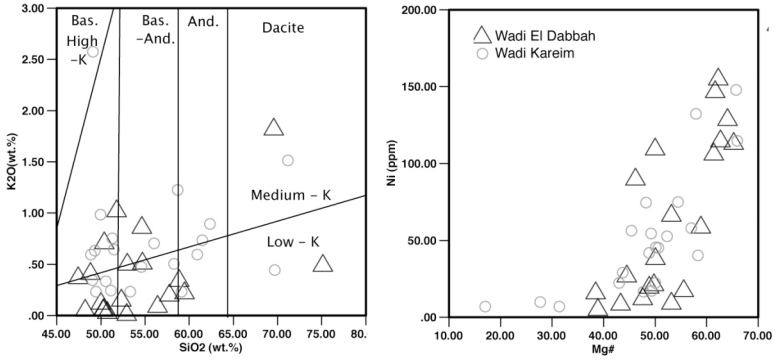

Figure 25: Chemical composition of YMV from Wadi Kareim and Dabbagh (Ali et al., in progress)

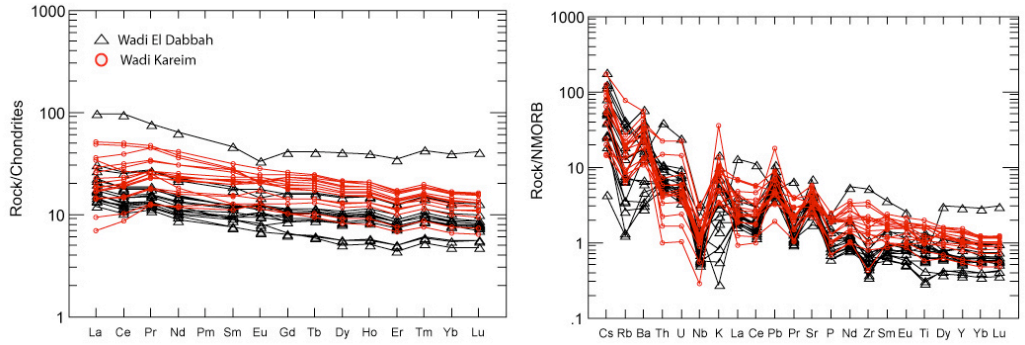

Fig. 26: Chondrite-normalized REE patterns for YMV from Wadi Dabbagh and Wadi Kareim (left) and MORB-normalized trace element diagrams (Right)

U-Pb zircon ages for these lavas give surprising results, with abundant pre-Neoproterozoic zircons as well as ~750 Ma zircons taken to approximate the age of eruption (Fig. 27 and 28). We do not think this results from contamination during

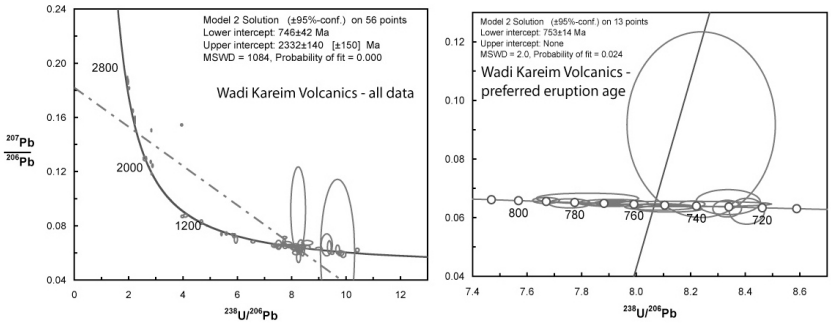

Figure 27 : SHRIMP-RG U-Pb zircon ages of YMV at Wadi Kareim (Ali, work in progress)

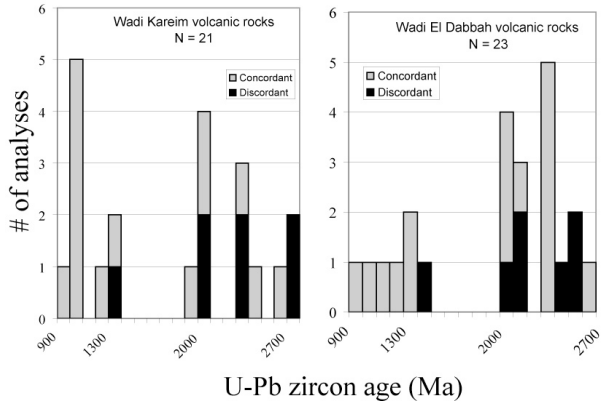

Figure 28: Histogram summarizing pre-ANS zircon ages for YMV samples from Wadi Kareim and Wadi Dabbagh (Ali, research in progress)

processing, particularly because the similar populations of old zircons are observed from multiple studies on either side of the Red Sea (Figure 29). Furthermore, some of these

samples were processed at the same time as a suite of 6 Egyptian granites, for which no pre-Neoproterozoic zircons were observed (Moussa et al., submitted). The abundance of pre-Neoproterozoic zircons in Neoproterozoic volcanics has also been observed by ion-porbe dating studies in Arabia (HargroveIII et al., 2006a; Kennedy et al., 2004). A similar distribution of pre-Neoproterozoic grains was found in Hammamat sediments from the NE Desert (Fig. 50) (Wilde and Youssef, 2002).

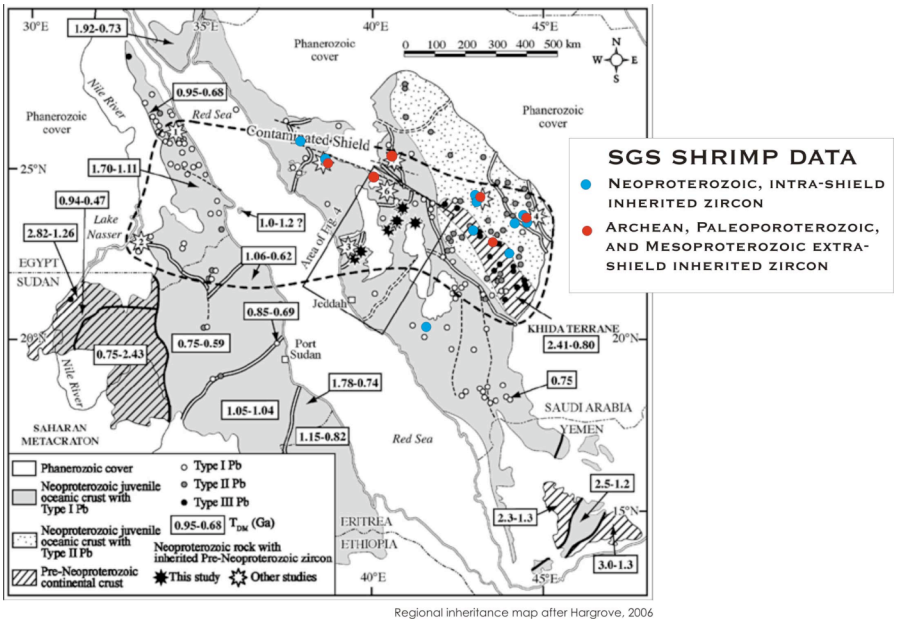

Figure 29: Distribution of samples from the Arabian-Nubian Shield containing significant pre-Neoproterozoic zircons. Original figure is from (HargroveIII et al., 2006b), with red and blue dots added by Johnson (personal communication, 2007)

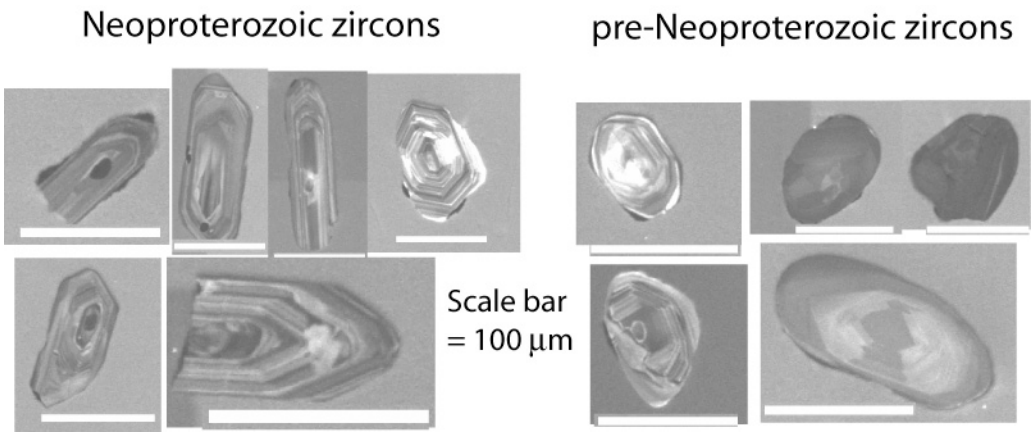

Figure 30: SEM-CL images of Neoproterozoic zircons (left) and xenocrystic pre-Neoproterozoic zircons (right) in samples of the YMV from Kareim and Dabbagh. Note that some of the older zircons are rounded, whereas Neoproterozoic zircons are euhedral (Ali, research in progress).

The abundance of pre-Neoproterozoic zircons in Neoproterozoic arc volcanics is puzzling, and how these became incorporated in juvenile arc-like melts may be

considered as **Controversy 13**. Perhaps these could have become incorporated as a result of sediments carried down into a subduction zone which then were carried back to the surface as melts but this explanation is not preferred. It seems much more likely that the were incorporated at crustal levels, either by interaction with pre-existing older continental crust **(**see **Controversy 1)** or continent-derived sediments deposited on oceanic crust. Zircon shapes provide an interesting clue (Figure 30). Some of the older zircons are rounded, consistent with recycling in sediments before being incorporated in the volcanics, but other old xenocrystic zircons show no rounding. This suggests that at least some of the older, xenocrystic zircons were recycled from sediments.

Controversy 14 concerns the significance of one of the most distinctive basement units, the Atud diamictite. This was previously called the Atud conglomerate but the unit clearly fits the description of diamictite (Stern et al., 2006). The term diamictite was introduced by (Flint et al., 1960) for lithified, poorly-sorted, non-calcareous terrigenous sedimentary rocks, from the Greek *diamignymi* meaning 'to mingle thoroughly'. Diamictites are poorly sorted breccia-conglomerates that can form in many ways – for example as debris flows and as impact ejecta, as well as due to the actions of glaciers. Tectonic and volcanic activity that formed the ANS provided many opportunities to produce diamictites without glaciers. Diamictites that result from glacial activity encompass a variety of peri- and subglacial environments, including terminal and lateral moraines deposited in both marine and subaerial environments, although marine diamictites are more likely to be preserved. The most unequivocal evidence for a glacial origin of a diamictite is

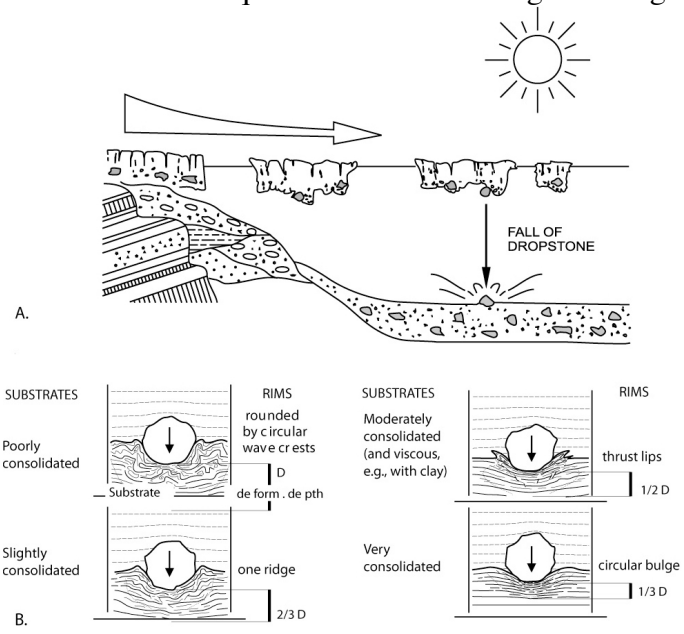

Figure 31: Formation of glaciogenic diamictites in a near-glacial aqueous environment, from Stern et al. (2006). A. Continental glacier erodes rock and transports this to a lake or to the sea. Icebergs form as glacier calves and drifts with the current, carrying embedded rocks. Melting iceberg eventually releases embedded rocks, which fall to lake or sea floor, impacting sediments and forming dropstones. B. Results of dropstone experiments where the consolidation of the substrate is varied, from poorly to very lithified. Note that the intensity and depth of deformation of substrate increases with decreasing substrate lithification, as a function of the diameter of the dropstone (D).

the identification of scratch marks on clasts or recognition of dropstones, but these are unlikely to be preserved in pre-600 Ma ANS basement sequences, which are invariably highly deformed. The most convincing evidence of glacial origin for a diamictite in the ANS is huge clast sizes with multiple lithologies that includes a lot of pre-Neoproterozoic material, because this is very difficult to accomplish without transport by ice.

The Atud diamictite contains a large diversity of lithologies, shapes, and sizes (heterolithologic breccias; figure 32). It has been recognized for 25 years that Atud Conglomerate contains granitic cobbles with pre-Neoproterozoic U-Pb zircon ages, which (Dixon, 1981) inferred to have been transported hundreds of kilometers from sources that now lie west of the Nile. Because of uncertainty surrounding the origin of ANS diamictites, breccias that contain only a single clast type (volcanic, plutonic, or sedimentary) are less likely to be of glacial origin. Some monomict diamictites may well have been deposited by glacial action, but the recognition of limited provenance makes it more likely that such deposits formed by non-glacial debris flows. No breccias inferred to have formed by meteorite impact are yet reported from Neoproterozoic units of the ANS.

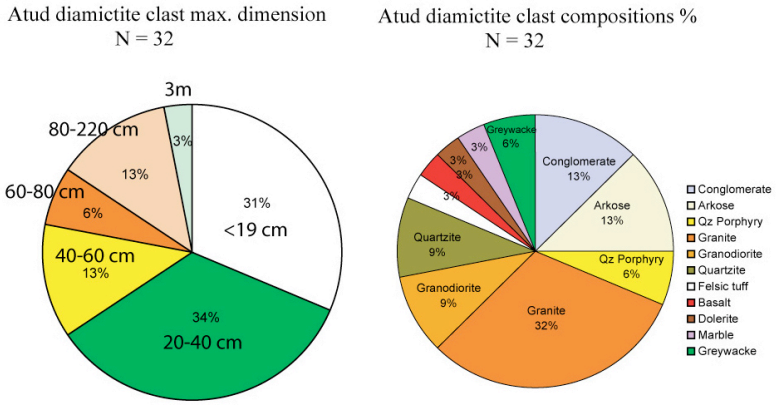

Figure 32 : Maximum sizes (left) and lithologies (right) of 32 Atud diamictite clasts from Wadi Kareim and Wadi Mobarak (Ali, research in progress)

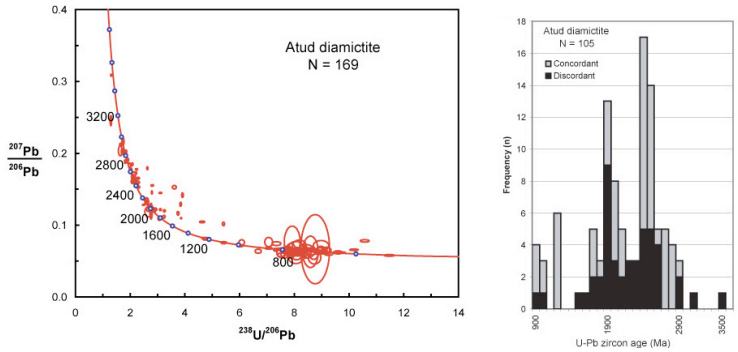

Figure 33: SHRIMP-RG U-Pb zircon ages for samples of clast and matrix of Atud diamictite from Wadi Kareim and Wadi Mobarak. Left figure shows all data, not concentration ~750 Ma. Right figure shows histogram of pre-Neoproterozoic concordia and $^{207}Pb/^{206}Pb$ ages, note concentration ~ 1.9 and 2.5 Ga (Ali, research in progress).

The Atud diamictite contains clasts with a wide range of sizes, compositions, and ages. Many of the ages are Neoproterozoic ~720-800 Ma but clasts of Paleoproterozoic to NeoArchean granite and quarzite are also common (Fig. 33). Distinctive arkose clasts

contain ancient as well as ~720 Ma zircons, as does the diamictite matrix. These arkose/microcongomerate clasts are common but similar units have not been found in place. These indicate that there was an earlier cycle of erosion-deposition-lithification prior to the one that formed the Atud diamictite itself.

A similar range in clast sizes, compositions, and ages is observed for the Nuwaybah diamictite (Zaam Group), Arabia, and these units are almost certainly correlative.If we accept that the coarsest metasediments are probabley glacial, we must also entertain the possibility that other parts of the clastic metasedimentary section may be partially glacial. The metasediments in Egypt are traditionally considered to be volcaniclastic, largely because these are wackes, are often turbidites with graded bedding, and are associated with arc-like sequences (Stern, 1981). One possibility is that these wackes were derived from two principle sources, one being arc-related sedimentation, the other being glacio-marine. **Controversy 15** concerns the extent to which the metasedimentary sequence is juvenile (arc-related) vs. glaciogenic, and can be resolved by ion-probe dating of zircons from these sediments.

Another diagnostic sedmentary unit in the CED is banded iron formation (BIF). BIF is not found in rocks younger than Archean and Paleoproterozoic but are found again in Neoproterozoic time. There are excellent BIF in Egypt (Sims and James, 1984) and Arabia (Goldring, 1990), and these examples of "ANS-BIF" may be correlative. These deposits are the subject of Ph.D. research by Mr. Sumit Mukherjee at UTD.

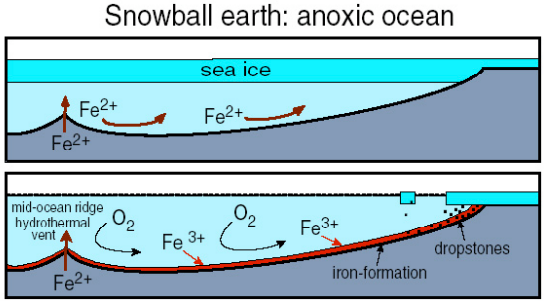

Fig. 34: Model for formation of Neoproterozoic banded iron formations (BIF). A) Snowball Earth: anoxic ocean. Ice covering ocean surface isolates seawater from mixing with atmosphere, cutting off the source of oxygen. Oxidation of organic matter consumes oxygen dissolved in seawater, with the result that seawater becomes anoxic and reducing. Iron introduced as Fe^{2+} at mid-ocean ridge hydrothermal vents remains in solution, causing a buildup of Fe^{2+} in seawater. B) Deglaciation: ocean ventilation. Melting of ice allows mixing of atmosphere and seawater, re-oxygenating seawater. Increased oxygen concentrations in seawater oxidizes Fe^{2+} dissolved in seawater to Fe^{3+}. This forms insoluble iron-oxides and is deposited as BIF on the seafloor. Modified from fig. 8 in http://www-eps.harvard.edu/people/faculty/hoffman/snowball_paper.html

Consideration of BIF through time led (Jacobsen and Pimentel-Klose, 1988) to conclude that Archean and Paleoproterozoic BIF had dominantly hydrothermal (mantle) sources, whereas Neoproterozoic BIF was mostly derived from continental weathering. Mr. Mukherjee's Nd-isotopic studies now in progress indicate this simple view is incorrect, and it appears that ANS-BIF was dominantly of hydrothermal origin. We may

consider the question of the origin of ANS-BIF as **Controversy 16**.

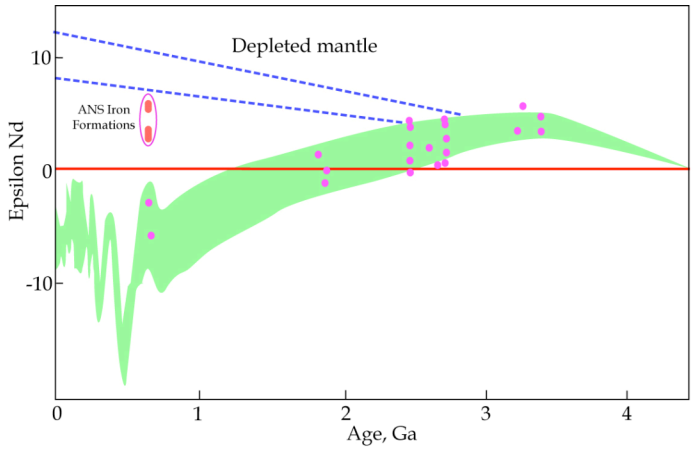

Figure 35: Plot of Epsilon-Nd versus age for BIF, modified by Mukherjee (in progress) after (Jacobsen and Pimentel-Klose, 1988), who reported the isotopic composition of Nd for 8 BIFs ranging in age from 0.65 to 3.4 Ga. They concluded that the Nd isotopic signature of BIFs changed from a principally mantle (hydrothermal) source in the Archean to Paleoproterozoic to a dominantly continental source in younger rocks. The data for 12 ANS BIFsamples (Mukherjee, PhD research in progress) contradicts this suggestion, instead suggesting a strong hydrothermal input for ANS-BIF.

Day Four: Today we will take a brief visit to look at rocks west of Marsa Alum. As of the time that this field guide is being assembled, no definite plan has been formulated. Possible targets include: 1) Magma mingling in granodiorites immediately west of the coastal plain; 2) Bereriq- Ghadir ophiolites, or 3) Atud diamictite at the type locality.

Fig. 36: Google Earth image of the Central Eastern Desert west of our hotel north of Marsa Alam.

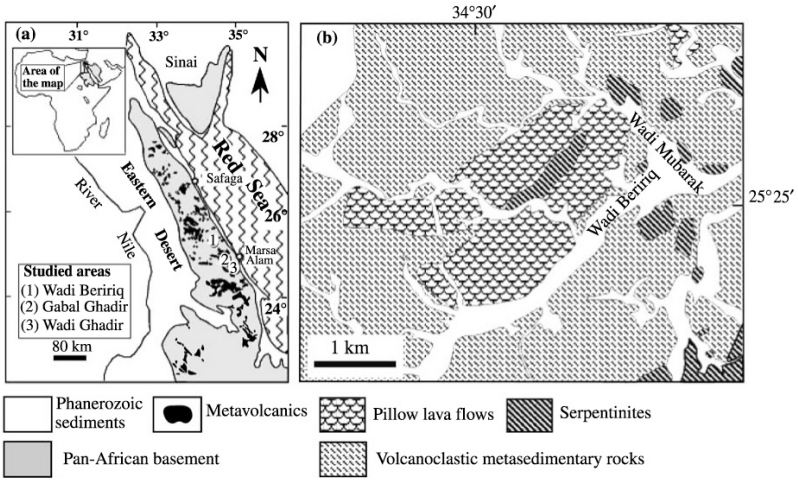

Fig. 37: A) Map showing the distribution of the metavolcanic rocks in the Eastern Desert of Egypt and localities studied by (Farahat et al., 2004) . Insert shows location of the Arabian-Nubian Shield (ANS). B) Geological map of Wadi Beririq area (Farahat et al., 2004).

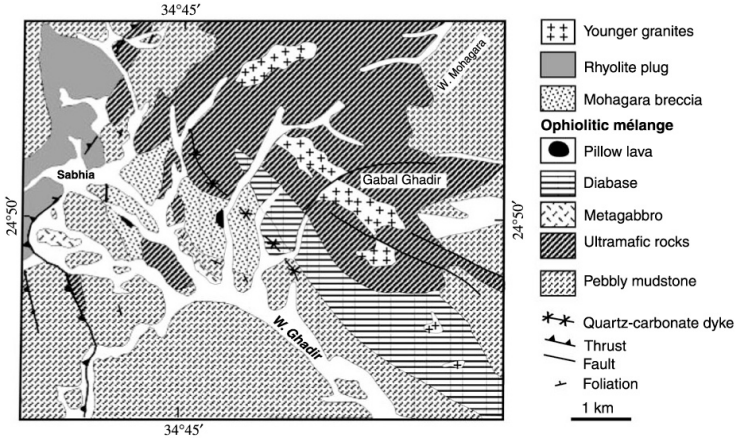

Fig. 38: Map showing the geology around the Gebel Ghadir ophiolite (Farahat et al., 2004). Location in Fig. 37A.

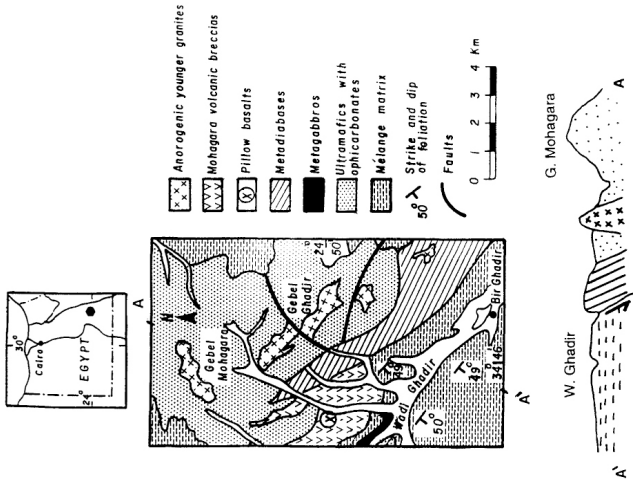

Fig. 39: Geologic relations around Gebel Ghadir ophiolite, from (Surour and Arafa, 1997)

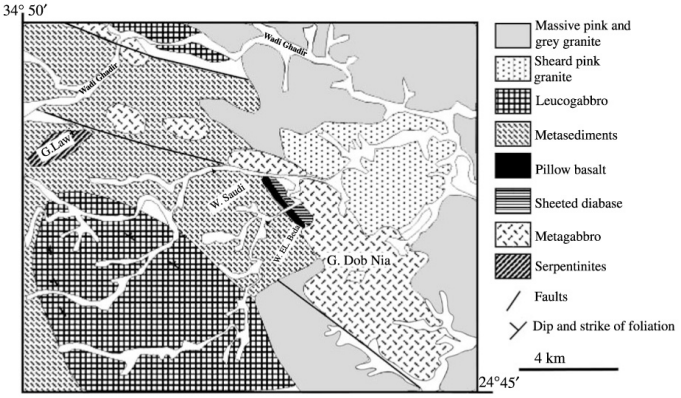

Fig. 40: Geologic relations around Wadi Ghadir ophiolite, from (Farahat et al., 2004). Location in Fig. 37A.

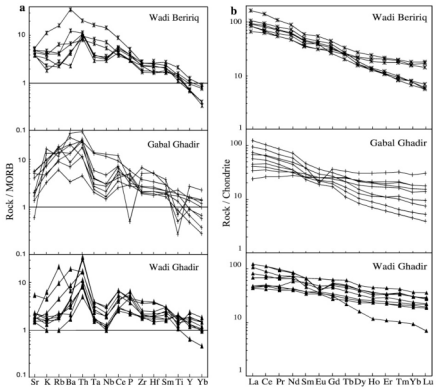

Fig. 41: Extended trace element patterns for Beririq-Ghadir ophiolites (left), REE patterns (right), from (Farahat et al., 2004).

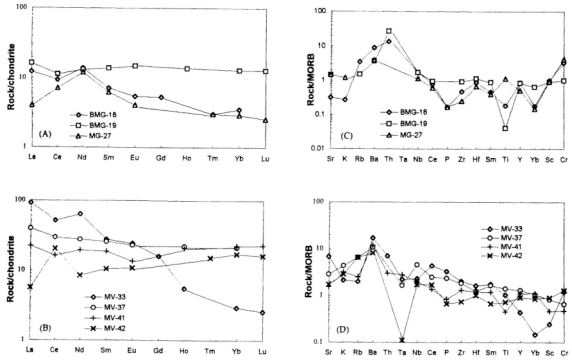

Fig. 42: REE patterns (left) and extended trace-element diagrams (right) for Fawkhir gabbros (upper) and pillowed basalts (lower), for comparison with data for Beririq-Ghadir ophiolites. Figure from (El-Sayed et al., 1999)(see Fig. 18 for location. How can ophiolitic ultramafics with such depleted spinels as found in Fig. 17B be associated with such enriched basalts and gabbros? This quandry was noted by (Stern et al., 2004)

for ophiolites of the entire ANS and may be considered as ***Controversy 17.***

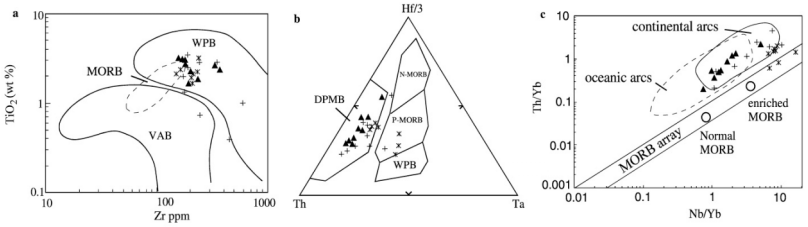

Fig. 42: Beririq-Ghadir ophiolites discrimination diagrams. A) TiO2 vs. Zr (Pearce, 1982), B) Hf/3–Th–Ta (Wood et al., 1979) and C) Th/Yb vs. Nb/Yb (Pearce and Peate, 1995) tectonomagmatic discrimination diagrams. MORB =mid-oceanic ridge basalt; WPB =within-plate basalt; VAB= volcanic-arc basalt. Symbols as in Fig. 41, from (Farahat et al., 2004).

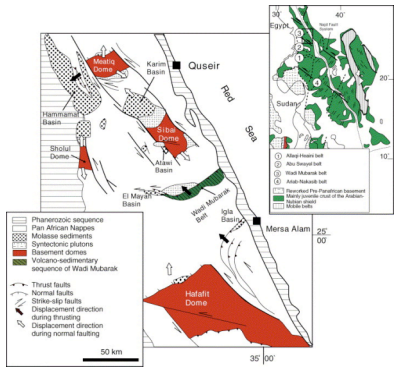

Fig. 43: Tectonic map of the Central Eastern Desert showing the core complexes, the northwest–southeast striking Najd fault system and the location of the Wadi Mubarak belt (modified after (Shalaby et al., 2005)). The inset shows the Najd Fault System and other deformation belts in the Arabian–Nubian Shield.

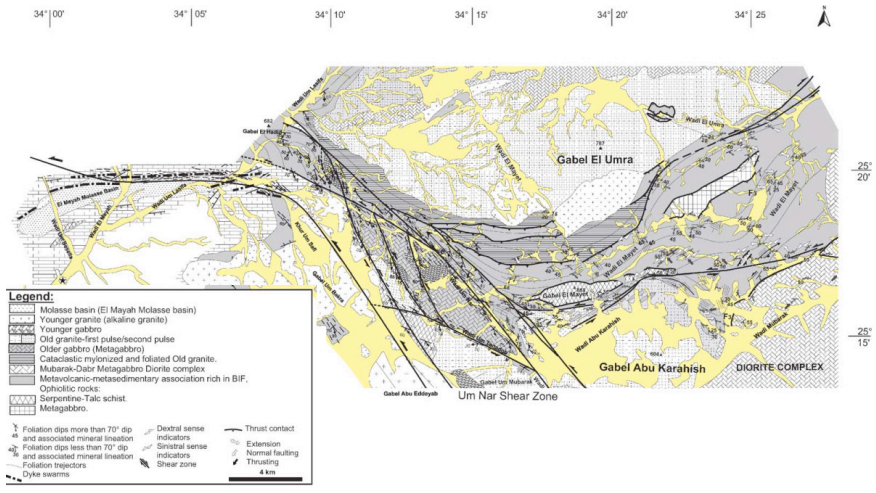

Fig. 44. Geological map of the Wadi Mubarak belt after (Shalaby et al., 2005). The Gabel El Umra granite complex (granodiorite to tonalite with abundant deformed

amphibolite and metavolcanic enclaves) bounds the Wadi Mubarak belt north of the northern thrust. It has an oval shape extending east–west for about 20 km. (Shalaby et al., 2005) recognized up to three separate intrusion stages within the complex. Two samples were dated using U–Pb zircons, giving 690±21 Ma and 654±5 Ma. The structural evolution is characterized by early NW-directed transport that formed several major thrusts. This event is correlated with the main deformation event in the Eastern Desert, elsewhere known as D2 (Shalaby et al., 2005). During this event the regional fabric of the Wadi Mubarak belt was wrapped around the El Umra granite complex in a west–east orientation. The Wadi Mubarak belt was subsequently affected during D3 by west–east and northwest–southeast trending sinistral conjugate strike–slip shear zones related to the formation of the Najd Fault System. D3 consisted of an older and a younger phase that reflect the change of transpression direction from ESE–WNW to ENE–WSW. The Umra granite intruded prior to D2 and the structural pattern of the Wadi Mubarak belt was initiated early during D2 (Shalaby et al., 2005).

Day Five: Today we will leave Marsa Alum early and return to Hughada. There we will head west to visit the area between Gebel Dokhan and Gebel Gattar. This is a very beautiful and instructive region in the NE Desert (Fig. 45), which is characterized by an

Fig. 45: Geologic map of the NE Desert, from (Ghanem et al., 1973). Granodiorites are blue 'X's, younger granites are white '+'s, Dokhan volcanics are brown 'v's, metavolcanics of unknown age are green lines, gabbros are red 'L's.

absence of ophiolites, BIF, diamictite, and other diagnostic lithologies of the CED. The NED also lacks evidence for Najd strike-slip faulting and instead has abundant bimodal dike swarms which indicate NW-SE directed extension (Fig. 46). (Stern, 1985) originally suggested that extension in the NED and adjacent areas caused Najd faulting, but it seems more likely that terminal collision between E and W Gondwana resulted in "escape tectonics", causing both Najd strike-slip faulting and NED extension (Burke and Sengör, 1986). The relationship between NE Desert extension and Najd strike-slip

faulting may be considered as **Controversy 18**. The extensional regime as reflected by the dike swarms encompassed ~60 Ma of time and at least 4 distinct generations of dikes are documented in southern Israel (Katzir et al., 2007). Similar dike swarms are common in Sinai (El-Sayed, 2006; Fritz-Töpfer, 1991) and Jordan (Jarrar et al., 2004; Jarrar et al., 2003) as well, and probably exist in NW Arabia. At present the different generations of dikes has not been worked out for the NE Desert. Where their geochemistry has been studied in detail in Sinai and Israel, these dikes record the evolution of the mantle from one that was strongly affected by subduction-related metasomatism ~600 Ma to a mantle with strong "within-plate" affinities ~540 Ma (Fritz-Töpfer, 1991; Katzir et al., 2007). The contact between the NED and CED is sharp and intrusive. Interestingly, there are no indications that a similar domain boundary exists in NW Arabia and the question of whether and how the NED-CED boundary continues on the other side of the Red Sea may be **Controversy 19**.

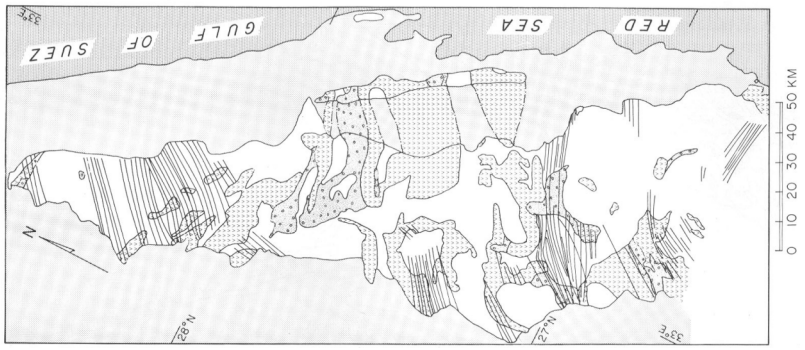

Fig. 46: Distribution of major lithologic units in the NE Desert, simplified after map of (Ghanem et al., 1973) (Fig. 45). Dokhan volcanics are 'v' pattern, Hammamat sediments are stippled, and dike trends are shown with lines. Subsurface extension (dashed) is inferred. Dike trends are from (Schürmann, 1966) and interpretation of Landsat MSS imagery (Stern et al., 1984).

The Qattar-Dokhan area is a good place to study the relationships between the Dokhan volcanics, bimodal dike swarms, Hammamat sediments, and Younger granites, all of which were developed about the same time ~600 Ma (Stern et al., 1984). Not only is it accessible, this is one of the prettiest regions in the Eastern Desert and also has a lot of Roman ruins. Gebel Dokhan in particular is the quarry which produced the beautiful "Imperial Porphyry" (Appendix 1). The beautiful purple color results from Mn-epidote withamite, which formed as a result of hyrothermal activity. We often forget that the term "porphyry" is from Latin and means "purple". Purple was the color of royalty, and the "Imperial Porphyry" was a deep brownish purple igneous rock with large crystals of plagioclase. Gebel Dokhan is the type locality of porphhry and porphyritic rocks.

A recent SHRIMP geochronology study of volcanic rocks from the type area of Gebel Dokhan (Wilde & Youssef 2000) has indicated SHRIMP U–Pb zircon ages of 602 ±9 Ma for the lower part of the sequence and 593±13 Ma for the Imperial Porphyry near the top of the unit (Wilde and Youssef, 2000).

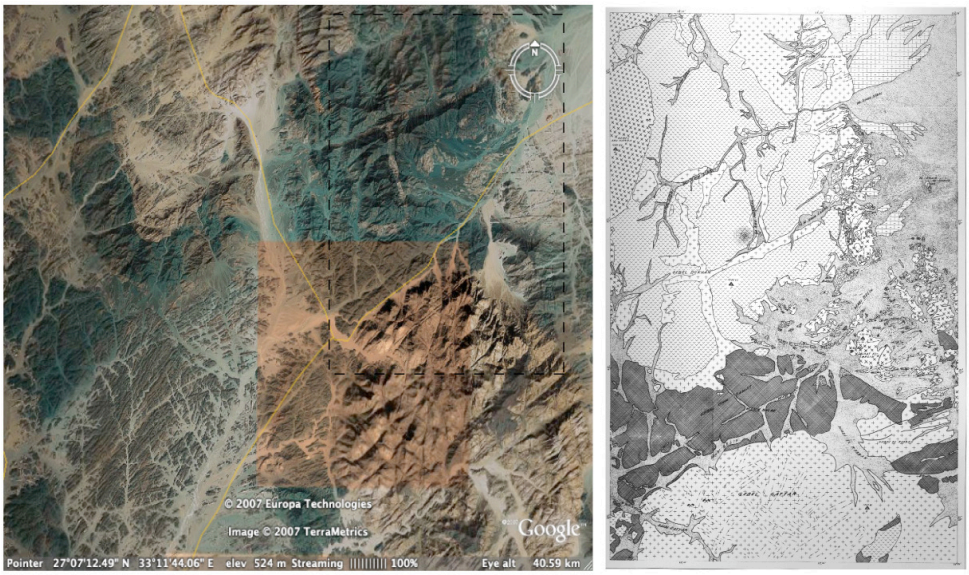

Fig. 47: Left: Google Earth image of area around Gebel Dokhan and Gebel Qattar. Dashed box shows location of geologic map on right, from (Ghobrial and Lotfi, 1967). Note NE-SW trending dike swarm west of Gebel Qattar. Note Gebel Qattar (Younger Granite) is in the south of the map, Gebel Dokhan (Dokhan Volcanics) is in the north, and Hammamat sediments define an E-W belt between granite and volcanics. The geochronological studies of (Willis et al., 1988) and (Wilde and Youssef, 2002) were carried out on these Hammamat sediments, and the geochronologic study of the Dokhan Volcanics of (Wilde and Youssef, 2000) was also done in this area.

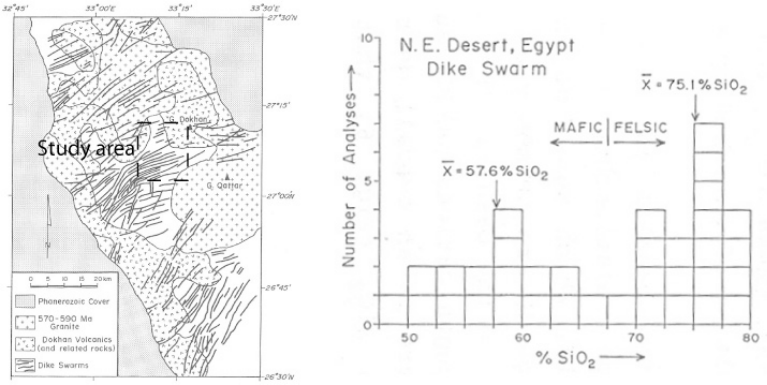

Fig. 48: Silica histogram (right) for dike swarms west of the Qattar-Dokhan area (left), from (Stern et al., 1988). Note bimodal distribution of compositions.

(Willis et al., 1988) studied ~400 m section (Fig. 49) and divided it into a lower half composed of massive polymict breccias and an upper half composed of sandstones, siltstones and shales. They concluded that the lower breecias were derived from the rapid uplift and erosion of a nearby 'ensimatic' terrane similar to that now preserved in the Central Eastern Desert to the south. Major and REE abundances indicated that the composition of the upper part of the Hammamat is similar to that of the upper continental crust.

Wilde and Youssef (2001) note "The view of Willis et al. (1988) is especially

confusing as, although the Dokhan Volcanic Series is stated to'conformably overlie' the Hammamat Group, it is also interpreted as providing detritus to the upper sequences of the Hammamat Group; an impossible scenario." I think that the Hammamat, Dokhan, and younger granites are broadly synchronous, so that the Dokhan and younger granite in places supplied detritus to the Hammamat and in other places the igneous rocks are clearly younger.

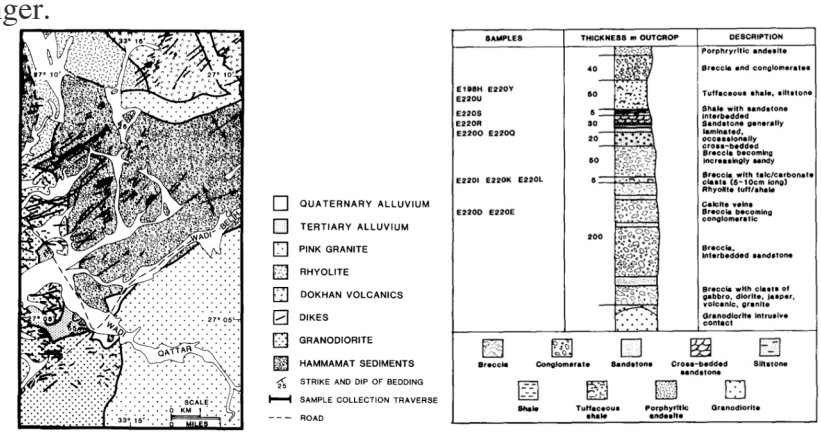

Fig. 49: Left: Location of Hammamat sediments studied by (Willis et al., 1988) (lower center of Fig. 47) and generalized stratigraphic section.

We may take a look at the Hammamat section here to see if the section might be overturned. Wilde and Youssef (2002) noted about the study of Willis et al. (1988) "No structural information was presented so it is unknown whether the sediments are inverted (as recognized inareas at Wadi Hammamat by Ries et al. (1983)), or whether the Dokhan Volcanic Series rocks are strictly interdigitated with the sediments, for it is impossible to explain the presence of Dokhan Volcanic clasts within the Hammamat sediments if the interpretation of Willis et al. (1988) is taken at face value." The relationship between the Hammamat and the Dokhan thus may be considered as **Controversy 19**.

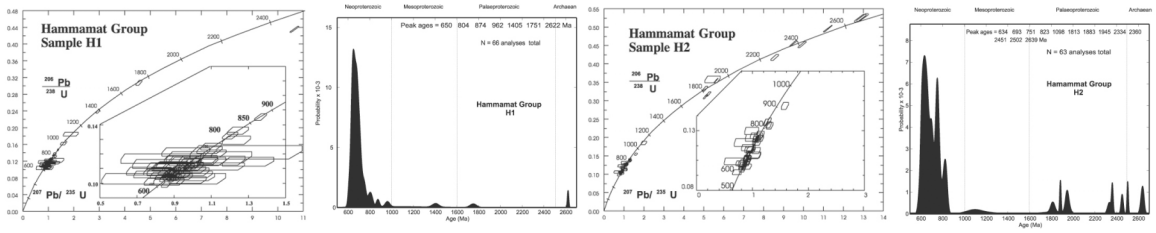

Fig. 50: Pairs of concordia-probability plots for samples of Hammamat sediments from Fig. 47 area. Note abundance of Paleoproterozoic and Neoarchean zircons, especially in sample H2. From (Wilde and Youssef, 2002). Compare distributions of older zircons with those shown in figs. 28 &33.

We have a good understanding of the age of the Hammamat in this region. (Willis et al., 1988) obtained a whole-rock Rb-Sr age of 585±15 Ma (MSWD = 2.0) which they took as approximating the age of sedimentation. The initial $^{87}Sr/^{86}Sr$ = 0.70323±13 indicated that these sediments were derived from juvenile crust. The untreated clay fractions gave an age of 643 ± 15 Ma (MSWD=2.4), suggesting some of the clay fraction was derived from older crust. (Wilde and Youssef, 2002) analyzed

detrital zircons from two samples of the Hammamat Group here (Fig. 50). H1 was from near the top of the sequence whereas H2 was from near its base. The sample from the top (H1) is dominated buy ~600 Ma zircons, whereas that from the base (H2) shows majorage peaks at 640 and 680 Ma; the former not previously identified as the time of major igneous activity in the North Eastern Desert. Both samples also contain older zircons particularly with Paleoproterozoic and NeoArchean ages; this contribution is also more significant at the base of the section (H2) than at the top (H1; Fig. 50). The origin and significance of these older zircons is not clear, as already indicated for controversies 13, 14, and 15. The abundance of older zircons in ~750 Ma sediments and volcanics in the CED suggests this crust may have contributed, as already suggested by Willis et al. (1988). Consequently, the inference of Wilde and Youssef (2002) that abundant older zircons indicates that the Hammamat was deposited by a continent-scale river system is thus not preferred by the writer of this field guide, although clearly the scale and direction of the Hamamamat drainage system may be considered to be **Controversy 20**.

It is also worth noting that detrital zircons from Cambro-Ordovician sandstones of southern Israel and Jordan show very similar age distributions (Fig. 51). A major difference is that in the Cambro-Ordovician sandstones there is a strong peak of ~1.0 Ga zircons, an age that is rarely observed in Neoproterozoic samples from Egypt but is more common in Neoproterozoic samples from Arabia. Crust of ~1.0 Ga age is unknown from the ANS or its flanks and is not encountered in the EAO north of Tanzania. **Controversy 21** concerns the source of 1.0 Ga zircons.

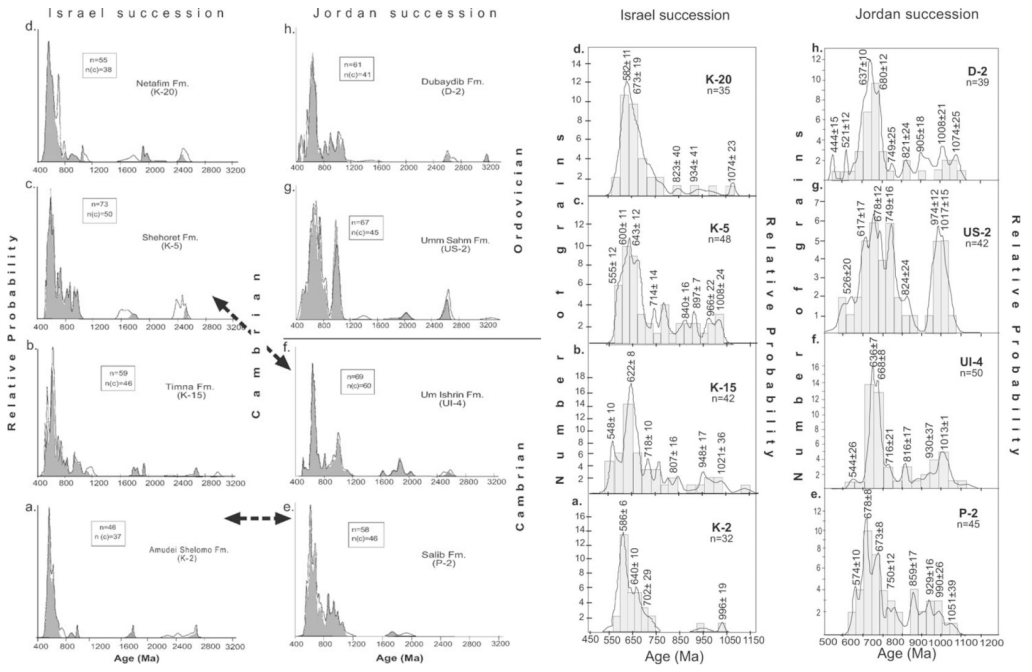

Fig. 51. Histogram showing age distribution of detrital zircons from Cambrian siliciclastic section of southern Israel and Jordan (Kolodner et al., 2006). Left: Relative probability histograms for all U–Pb SHRIMP ages of detrital zircons (Israel onleft, Jordan on right). The relative probabilities of weighted mean ages of all data are limited by the black curves, whereas the concordant ages histograms are filled grey. Arrows indicate correlative formations. Right: Expanded relative probability histograms for

concordant zircon ages younger than 1.2 Ga. The superimposed bar graphs indicate the results of mixture modelling, namely each age subgroup with its 95% confidence limits and relative abundance.

One wonders whether similar populations of pre-Neoproterozoic zircons would be found in the ~600 Ma Saramuj conglomerate of Jordan (Jarrar et al., 1991) or in sediments preserved in the post-accretionary basins of the Arabian Shield (Johnson, 2003). Would these reveal abundant 1.0 Ga zircons or would they be more like the Hammamat and lack ~1.0 Ga zircons?

Fig. 52 shows a cartoon of environments envisaged by (Stern et al., 1984) for the NE Desert at ~600 Ma. A strongly extensional environment was envisaged, but this interpretation often conflicts with interpretations for the tectonic environment in which the Dokhan volcanics were erupted. Fig. 53 shows the intimate relationship between Dokhan volcanics and younger granites at the type locality, such that the Dokhan volcanics seem to rest as a carapace on the younger granites.

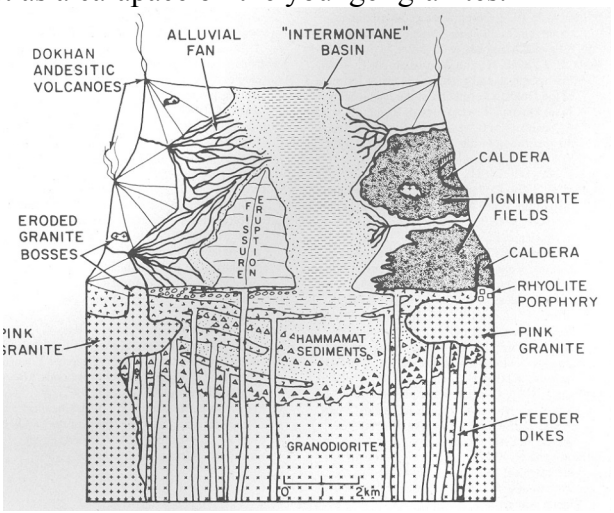

Fig. 52: Block diagram-cartoon illustrating the nature of crustal environments in the NE Desert at ~600 Ma. Perspective is down the axis of an E-W elongated depositional basin with flanking volcanic highlands. From (Stern et al., 1984)

There are several controversies about the Dokhan Volcanics. The first reflects Controversy 6, articulated above. Their trace element signatures indicate formation from a source that was modified by subduction-related fluids, with (Stern and Gottfried, 1986) argued these formed as a result of rifting, but other authors argue these formed at an Andean-type convergent plate margin. One of the best recent studies of the Dokhan Volcanics is that of (Eliwa et al., 2006), who studied the Dokhan Volcanics just north of the type locality (Fig. 52) and also summarized what was known about other Dokhan occurrences in the NED. Their high-quality data set and interpretations are referred to extensively below.

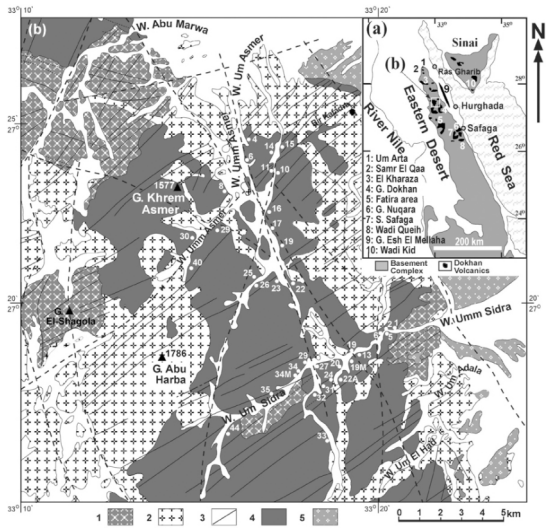

Fig. 53. (a) Distribution of the Dokhan Volcanics in the Eastern Desert and Sinai and (b) geological map of the Wadi Um Sidra and Wadi Um Asmer area, NED, Egypt (Eliwa et al., 2006). This map area lies on the north side of Gebel Dokhan on Fig. 47. Lithologies are: (1) Granodiorite-quartz diorite, (2) biotite hornblende granites and adamellite, (3) biotite granite, (4) perthitic granite, (5) granitic and granosyenite dykes, (6) diabasic dykes, (7) doleritic and dioritic dykes, (8) Dokhan Volcanics, (9) recent deposits. The numbers refer to their analyzed samples labeled AS and US along Wadi Um Asmer and Um Sidra, respectively.

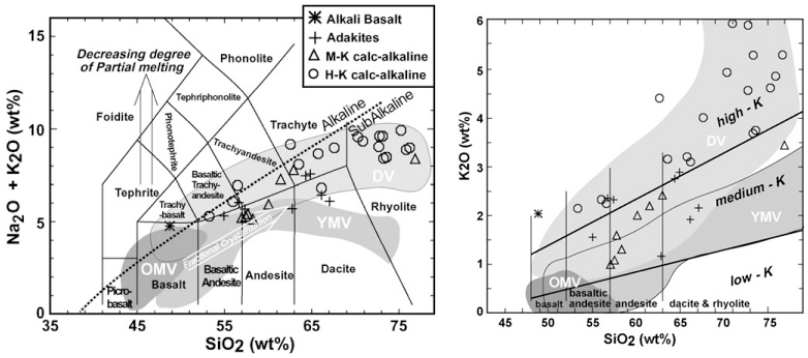

Fig. 54. Left: Geochemical classification of Dokhan Volcanics on the total alkalis-silica (TAS) diagram, from (Eliwa et al., 2006). Symbols show the compositions of that study. For comparison, fields are also shown for Older and Younger metavolcanics(OMV and YMV) from Stern (1981), and Dokhan Volcanics (DV) from other areas Right: SiO2 vs. K2O diagram. HK: high-K; MK: medium-K; CA: calc-alkaline; Alk Bas: alkali basalt; HK CA: high-K calc-alkaline volcanics; MK CA: medium-K calc-alkaline.

Eliwa et al. (2006) noted that the Dokhan Volcanics from Wadi Um Sidra and Um Asmer range from medium- to high-K alkali basalt to rhyolite. They comprise voluminous medium- to high-K calc-alkaline lavas, subordinate adakitic lavas, and minor alkali basalt. Adakitic lavas have steeper REE patterns with (LaN/LuN = 11.1–14.4), while calc-alkaline rocks have less fractionated REE patterns (LaN/LuN = 6.3–9.4. Adakitic lavas contain very low Y (<18 ppm) and heavy REE (HREE; Yb≤1 ppm)

contents, with high Sr (>750 ppm) and Sr/Y (>40). They also have high Cr and Ni and

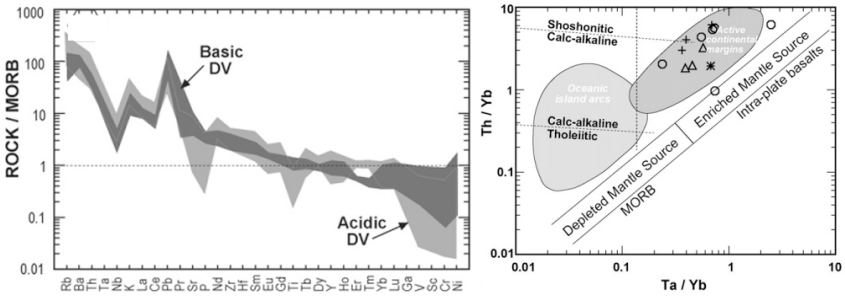

Fig. 55. Left: MORB-normalized extended trace element fields for mafic (basic)and felsic (acidic) Dokhan Volcanics studied by (Eliwa et al., 2006). Right: Th/Yb-Ta/Yb plot, showing that Dokhan volcanics plot above the "mantle array" as is typical of subduction-related convergent margins igneous suites.

low Nb, Rb, and Zr contents compared to coexisting calc-alkaline lavas. The steep REE patterns and moderately high Cr and Ni contents were noted by (Stern and Gottfried, 1986), who inferred that this resulted from generation of parental mafic magmas by melting garnet peridotite, followed by moderate fractionation. Eliwas et al. (2006) infer the presence of true adakites indicates the subduction of a hot oceanic ridge before collision between E and W Gondwana, with melting of the hot oceanic slab to form Dokhan adakites after collision.

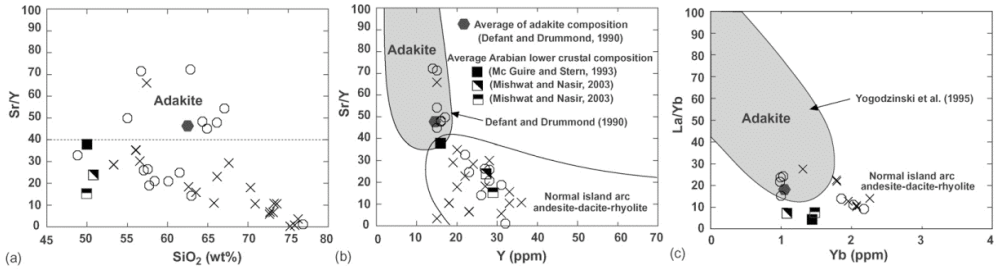

Fig. 55. Binary relations of adakites: (a) SiO_2 vs. Sr/Y, (b) Y vs. Sr/Y, and (c) Yb vs. La/Yb. Samples of Dokhan volcanics are plotted, from (Eliwa et al., 2006).

Part of the confusion about the tectonic setting where the Dokhan formed results from over-reliance on trace element compositions. Studies of the dike swarms, which clearly formed in a strongly extensional environment, indicate that the mantle "memory" of subduction-related metasomatism took several tens of millions of years to lose. Field studies of the dikes, intended to work out a relative chronology of emplacement, supported by U-Pb zircon geochronology and chemistry of the most primitive magmas, would provide a unique perspective on how subduction-metasomatised mantle loses this memory. It is important to note that the Dokhan volcanics were one of the first igneous sequences erupted after the orogenic-to-extensional "transition" shown in Fig. 6. It is to be expected that magmas derived from mantle that, until recently had been subjected to subduction-related metasomatism, would have some of the characteristics found for subduction-related magmas, such as Nb depletions and Pb spikes, as well as Th/Yb that is elevated from the mantle array (Fig. 55).

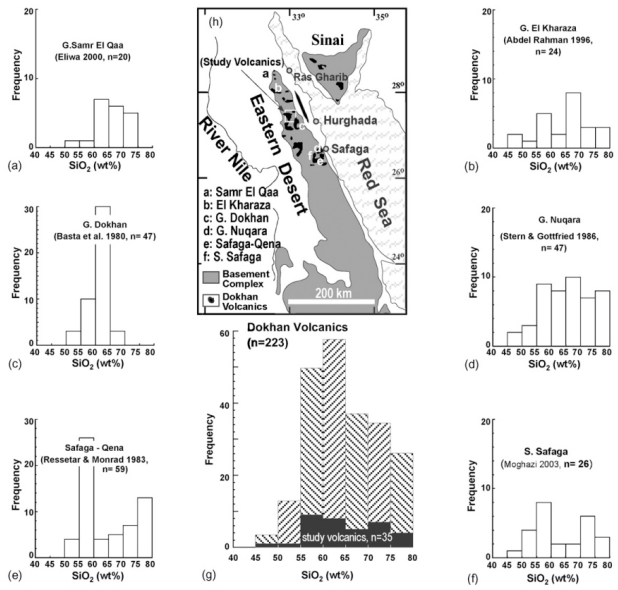

Fig. 56. Histograms showing SiO_2 (wt.%) for the Dokhan Volcanics from different areas in the NED: (a) G. Samr El Qaa; (b) G. El Kharaza; (c) G. Dokhan; (d) G. Nuqara; (e) Safaga-Qena road; (f) S. Safaga area; (g) the studied volcanics compared to data of the Dokhan Volcanics compiled herein, and (h) distribution map of the Dokhan Volcanics provinces used, (Eliwa et al., 2006).

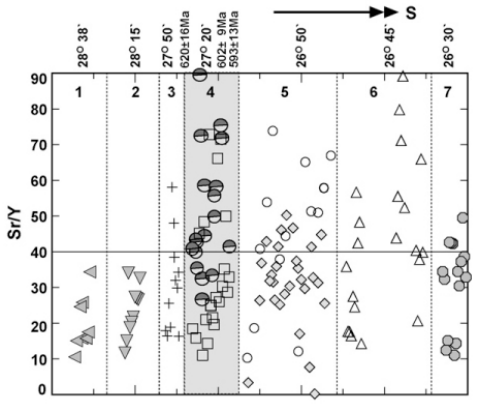

Fig. 57. Latitudinal distribution of Sr/Y in Dokhan Volcanics in the North Eastern Desert, from (Eliwa et al., 2006). (1) Umm Arta Volcanic, (2) G. Samr El Qaa, (3) G. Kharaza, (4) the studied area , (5) Fatira, (6) G. Nuqura, and (7) S. Safaga. Note the Sr/Y generally increases from north to south.

Finally, we must mention the younger granites; these are referred to by various names, especially "Younger Granites" and "Pink Granites". (Schürmann, 1966) called them the "Gattarian granites", but that name is not widely used. **Controversy 22** encompasses several controversies about their origin and significance. These granititic rocks can be usefully if not unequivocally compared to "A-type" granites, recently summarized by (Bonin, 2007 in press). This term was coined first less than thirty years ago, and is variably taken to indicate "alkaline", "anorogenic", or "anhydrous". A-type

suites occur in geodynamic contexts ranging from within-plate settings and at extensional plate boundaries. Because they are relatively anhydrous, they can rise to shallow levels in the crust without solidifying. Consequently, they are usually emplaced at the subvolcanic level where they form ring complexes rooting caldera volcanoes. Characteristic features include abundant alkali feldspars, iron-rich mafic mineralogy, bulk-rock compositions yielding ferroan, alkali-calcic to alkaline affinities, high LILE+HFSE abundances, and pronounced anomalies indicating significant mineral fractionation. Isotopic features indicate a large mantle input. Experimental data show that A-type magmas contain dissolved OH–F-bearing fluids and yield high-temperature liquidus, favouring early crystallisation of anhydrous iron minerals, such as fayalite. Bonin (2007 in press) notes that though early petrogenetic models concluded that A-type granitic melts are generated by melting of the lower crust, this interpretation is increasingly rejected in favor of an origin by magmatic differentiation of mantle-derived melts. No convincing A-type liquids have been produced experimentally from crustal materials, nor have any leucosomes of A-type composition been detected within migmatitic terranes. Bonin (2007) observes that, because A-type granitic rocks are associated with mafic igneous rocks on the continents as well as on the ocean floor, A-type granite is likely to come from mantle-derived transitional to alkaline mafic to intermediate magmas. He outlines a multi-stage fractionation scenario for the origin of A-type granitic magmas (Fig. 58).

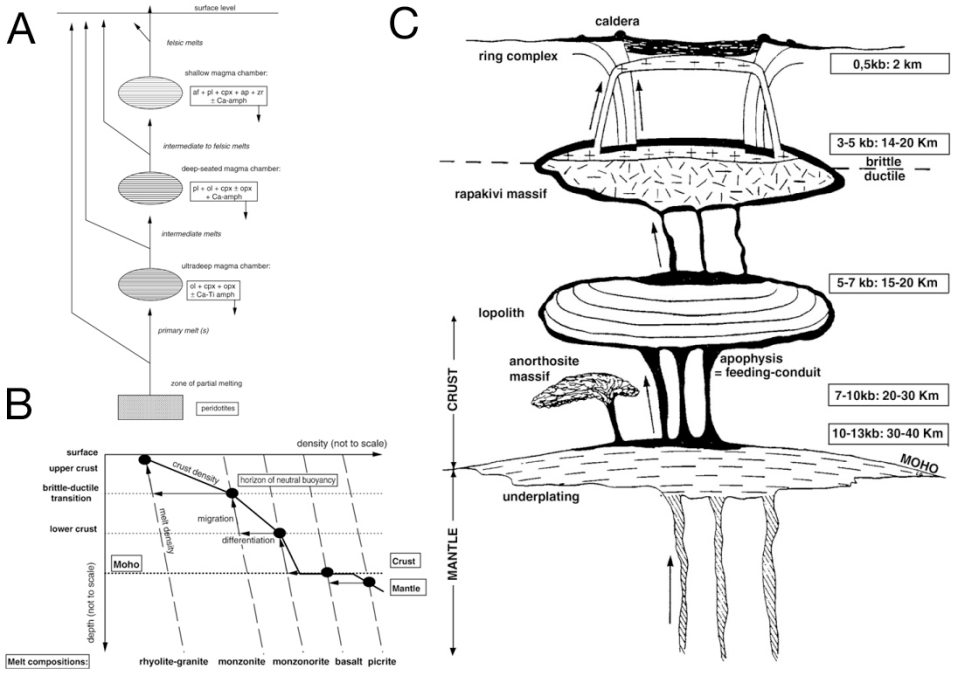

Fig. 58: General models for the origin of A-type granitic magmas (Bonin, 2007 in press). A) Fractionation processes within a network of magma chambers emplaced at various depths. Primary magmas originate from partial melting of upper mantle and evolve ultimately into felsic residual liquids. At each level, the average fractionating mineral assemblage, which precipitates as cumulates, is specified. B) Density versus depths controlling A-type melt evolution within upper mantle and crust. In a strongly extensional environment, melts migrate upwards to a position of neutral buoyancy, where it differentiates further, yielding liquids of progressively lower density. C) Structural

levels of A-type granite magmatism. Depths are approximate. Surface level: caldera volcano, feeder radial and ring dykes, and domes. Subvolcanic 1–4 km-deep level: ring complex, cone sheets, and dyke swarms. Intermediate 7–15 km-deep level: mixed cumulate-liquid rapakivi granite batholiths, and quartz-alkali feldspar cumulates. AMCG complex, 15–30 km-deep plutonic level: mafic to intermediate layered lopoliths from which felsic residual liquids can escape, and associated massif anorthosite complexes. Underplating zone at the 30–40 km-deep mantle-crust boundary: ultramafic layered sheets. Though inappropriate, the term 'underplating' is maintained because it is widely used, 'intraplating' would be more adequate. Partial melting zones are located at greater depths within upper mantle.

Global syntheses of A-type granites tend to overlook the abundance of these rocks in the northern ANS. This is partly because the concept has only recently been adopted by researchers in the region and by the fragmented nature of granite research around the Red Sea. Nevertheless, what (Bentor, 1985) called the Katherina Province is huge; he identified it as encompassing >15 million km^2, and identified it as "...possibly the largst igneous province known." For this reason alone, it will be useful to identify the northern ANS A-type province (590±20Ma) as a natural laboratory for studying the many manifestations of these igneous rocks, as this may attract the research interest of international scientists and foster collaboration among scientists in the region. The A-type granites of the region are also significant economically, because extreme fractionates contain greatly elevated abundances of REE, U, Th, and rare metals W-Ta-Nb.

The general observations of Bonin (2007 in press) are true for A-type granites of the northern ANS, which have mantle-like isotopic compositions of Sr and Nd, are often associated with comagmatic mafic plutonic rocks, and were emplaced at shallow levels (sometimes associated with felsic tuffs and caldera complexes). The oxygen isotopic composition of zircons in the 593±16 Ma (Rb-Sr whole rock) Katherina pluton in Sinai were determined recently (Katzir et al., 2007 in press). They noted that two size fractions of zircon have indistinguishable and homogeneous $\delta^{18}O$ of 5.82± 0.06‰. The $\delta^{18}O$ value of the syenogranite zircon only mildly exceeds the oxygen isotope range of mantle zircon (5.3±0.3‰), and the observed difference of +0.5‰ can be accounted for by magmatic fractionation. Katzir et all (in press) conclude that the ultimate source of the Katharina granitic magma should thus be sought in mantle-derived sources.

The younger granites formed after the collision between E and W Gondwana (Fig. 6) but do not appear to be anatectic melts of thickened crust. Most of these granitic rocks are undeformed but those emplaced in active Najd shear zones or associated with core complexes are very deformed. Most Egyptian younger granites and correlatives in Israel, Jordan, and perhaps northern Arabia are concentrated at the northern limits of the ANS but similar granites are found in the southern ANS, including the ~610 Ma Mereb granites of northern Ethiopia and Eritrea (Miller et al., 2003). It is not clear what is the significance of this spatial distribution but it may have required a large amount of extension to accommodate these magmas, depending on whether they are anatectic melts of the lower crust or fractionates of mafic magma. If these granites from by crustal anatexis, little additional space may be required because mass is transferred from lower to upper crust. In the case of fractionation, a large amount of space must be created to allow mantle-derived magmas to pool and fractionate. The preponderance of evidence is

that 590±20 Ma ANS A-type granitic rocks formed by fractionation of mafic or intermediate precursors, requiring a large amount of extension.

ANS A-type granitic rocks are characterized by REE patterns with large depletions in Eu and flat patterns for the heavy REE, precluding a role for garnet residua or fractionates and requiring an important role for feldspar residua or fractionates. Most researchers agree that these granitic rocks formed by fractionation of mafic parental magmas ((Beyth et al., 1994; Jarrar et al., 2003; Kessel et al., 1998; Moghazi, 1999; Stern and Gottfried, 1986). Jarrar et al. (2003) concluded that the ~600-560 Ma Araba suite plutonic rocks of Jordan included A-type granites that were derived by extreme fractional crystallization (~80%) of mafic to intermediate magmas. Such igneous rocks are common in the Jordanian basement, where the Araba Mafic to Intermediate Suite (48–65% SiO_2) comprises quartz-diorites, quartz-monzodiorites, monzodiorites and monzogabbros.

Although it is increasingly clear that magmagenesis of ANS A-type granitic rocks was dominated by fractionation, the details of this process are unresolved. Additional processes are required by the observed enrichment of HREE relative to LREE in some of these granites and by abrupt increases in Nb, Y, U over a restricted range of SiO_2 (Katzir et al., 2007 in press). Moghazi (1999) emphasizes the F-enrichment of some ANS A-type granites, emphasizing that F-rich fluids can cause HREE and HFSE enrichments due to F complexing in the late stages of evolution of a granitic melt. The possibility of magma immiscibility also warrants careful consideration (Stern and Voegeli, 1987).

The relationship between A-type granitic magmatism and core-complex provides excellent opportunities for structural geologists, petrologists, and geochronologists can interact to provide important new insights. In this fashion, Fritz et al. (2002) integrated structural studies with Ar-Ar thermochronology and concluded that exhumation of the Meatiq, Sibai, and Hafafit core complexes in the CED was facilitated by continuous magmatism, which greatly weakened the crust. This contrasts with the relationship between extension and younger granite magmatism is in the NED and Jordan, where an intimate association of the granitic plutons with bimodal dike swarms is observed. Perhaps the Wadi Kid core complex in Sinai preserves a stage intermediate between core-complex extension and dike swarm extension, or perhaps an intermediate stage in Jordan or NW Arabia preserves such a relationship.

Abdeen, M.M. and Greiling, R.O., 2005. A quantitative Sructural Study of Late Pan-African Compressional Deformation in the Central Eastern Desert (Egypt) During Gondwana Assembly. Gondwana Research, 8: 457-471.

Abdel-Rahman, A.M., 1996. Pan-African volcanism: Petrology and geochemistry of the Dokhan Volcanic suite in the northern Nubian Shield. Geological Magazine, 133: 17-31.

Abdelsalam, M.G., Abdeen, M.M., Dowaidar, H.M., Stern, R.J. and A.A.Abdelghaffar, 2003. Structural evolution of the Neoproterozoic Western Allaqi-Heiani suture, southeastern Egypt. Precambrian Research, 124: 87-104.

Ahmed, A.H., Arai, S. and Attia, A.K., 2001. Petrological characteristics of podiform chromitites and associated peridotites of the Pan African ophiolite complexes of Egypt. Mineralium Deposita, 36: 72-84.

Azer, M.K. and Khalil, A.E.S., 2005. Petrological and mineralogical studies of Pan-African serpentinites at Bir Al-Edeid, Central Eastern Desert, Egypt. J. African Earth Sci., 43: 525-536.

Azer, M.K. and Stern, R.J., 2007 in press. Neoproterozoic (835-720 Ma) serpentinites in the Eastern Desert, Egypt: Fragments of fore-arc mantle. Journal of Geology.

Bakor, A.R., Gass, I.G. and Neary, C.R., 1976. Jabal al Wask, northwest Saudi Arabia: an Eocambrian back-arc ophiolite. Earth and Planetary Science Letters, 30: 1-9.

Bennett, J.D. and Mosley, P.N., 1987. Tiered-tectonics and evolution, E. Desert and Sinai, Egypt. In: G. Matheis and H. Schandelmeier (Editors), Current Research in African Earth Sciences. Balkema, Rotterdam, pp. 79-82.

Bentor, Y.K., 1985. The crustal Evolution of the Arabo-Nubian Massiif with Special Referece to the Sinai Peninsula. Precambrian Research, 28: 1-74.

Beyth, M., Stern, R.J., Altherr, R. and Kröner, A., 1994. The Lae Precambrian Timna Igneous Complex, southern Israel: Evidence for comagmatic-type Sanukitoid Monzodiorite and Alkali Granite magma. Lithos, 31: 103-124.

Blasband, B., White, S., Brooijmans, P., DeBoorder, H. and Visser, W., 2000. Late Proterozoic extensional collapse in the Arabian-Nubian Shield. J. Geol. Soc. London, 157: 615-628.

Bonin, B., 2007 in press. A-type granites and related rocks: Evolution of a concept, problems and prospects. Lithos.

Botros, N.S., 2004. A New Classification of the Gold Deposits of Egypt. Ore Geology Reviews, 25: 1-37.

Burke, K. and Sengör, C., 1986. Tectonic escape in the evolution of the continental crust. In: M. Barazangi and L. Brown (Editors), Reflection Seismology: The Continental Crust. AGU, Washington DC, pp. 41-53.

Dixon, T.H., 1981. Age and chemicla characteristics of some pre-Pan-African rocks in the Egyptian Shield. Precambrian Research, 14: 119-133.

El-Bouseily, A.M., El-Dahhar, M.A. and Arslan, A.I., 1985. Ore-microscopic and geochemical characteristics of gold-bearing sulfide minerals, El Sid Gold mine, Eastern Desert, Egypt. Mineralium Deposita, 20: 194-200.

El-Gaby, S., El-Nady, O. and Khudeir, A., 1984. Tectonic evolution of the basement complex in the Central Eastern Desert of Egypt. Geologische Rundschau, 73: 1019-1036.

El-Gaby, S., List, F.K. and Tehrani, R., 1988. Geology, evolution and metallogenesis of the Pan-African Belt in Egypt. In: S. El-Gaby and R.O. Greiling (Editors), The Pan-African belt of Northeast Africa and Adjacent Areas. Friedr Viewgsohn, Braunschweig/Wiesbaden, pp. 175-184.

El-Ramly, M.F., 1972. A new geological map for the basement rocks in the eastern and southwestern deserts of Egypt. Egypt Geol. Survey Annals, 2: 1-18.

El-Sayed, M.M., 2006. Geochemistry and petrogenesis of the post-orogenic bimodal dyke swarms in NW Sinai, Egypt: Constraints on the magmatic-tectonic processes during the late Precambrian. Chemie der Erde, 66: 129-141.

El-Sayed, M.M., Furnes, H. and Mohamed, F.H., 1999. Geochemical constraints on the tectonomagmatic evolution of the late Precambrian Fawakhir ophiolite, Central eastern Desert, Egypt. Journal of African Earth Sciences, 29: 515-533.

El-Sayed, M.M., Mohamed, F.H., Furnes, H. and Kanisawa, S., 2002. Geochemistry and Petrogenesis of the Neoproterozoic Granitoids in the Central Eastern Desert, Egypt. Chemie der Erde, 62: 317-346.

El-Sharkawy, M.A. and El-Bayoumi, R.M., 1979. The ophiolites of Wadi Ghadir area, Eastern Desert, Egypt. Annals of the Geological Survey of Egypt, 9: 125-135.

El-Sharkawy, M.F., 2000. Talc mineralization of ultramafic affinity in the Eastern Desert of Egypt. Mineralium Deposita, 35: 346-363.

Eliwa, H.A., Kimura, J.-I. and Itaya, T., 2006. Late Neoproterozoic Dokhan Volcanics, North Eastern Desert, Egypt: Geochemistry and petrogenesis. Precambrian Research, 151: 31-52.

Essawy, M.A., 1974. Atalla Felsite Intrusion and its neighbouring rhyolitic flows and tuffs, Eastern Desert. Annals of the Geological Survey of Egypt, 2: 271-281.

Farahat, E.S., Mahalawi, M.M.E., Hoinkes, G. and Aal, A.Y.A., 2004. Continental back-arc basin origin of some ophiolites from the Eastern Desert of Egypt. Mineralogy and Petrology, 82: 81-104.

Flint, R.F., Sanders, J.E. and Rodgers, J., 1960. Diamictite, a substitute term for symmictite. Geol. Soc. Am. Bull., 71: 1809-1810.

Fowler, A.-R. and Kalioubi, B.E., 2004. Gravitational collapse origin of shear zones, foliations and linear structures in the Neoproterozoic cover nappes, Eastern Desert, Egypt. Journal of African Earth Sciences, 38: 23-40.

Fritz, H. et al., 2002. Neoproterozoic tectonothermal evolution of the Central Eastern Desert, Egypt: a slow velocity tectonic process of core complex exhumation. J. African Earth Sciences, 34: 137-154.

Fritz-Töpfer, A., 1991. Geochemical characterization of Pan-African dyke swarms in southern Sinai: from continental marginto intraplate magmatism. Precambrian Research, 49: 281-300.

Ghanem, M., Dardir, A.A., Francis, M.H., Zalata, A.A. and Zeid, K.M.A., 1973. Basement rocks in Eastern Desert of Egypt north of latitude 16°40'N. Annals Geol. Surv. Egypt, 3: 33-38.

Ghobrial, M.G. and Lotfi, M., 1967. The Geology of Gebel Gattar and Gebel Dokhan areas, Geological Survey of Egypt 40.

Goldring, D.C., 1990. Banded iron formation of Wadi Sawawin district, Kingdom of Saudi Arabia. Trans. Instn. Min. Metall. (Sec. B Appl. earth sci.), 99: B1-B14.

Greiling, R.O. et al., 1994. A structural synthesis of the Proterozoic Arabian-Nubian Shield in Egypt. Geologische Rundschau, 83: 484-501.
HargroveIII, U.S., Stern, R.J., Griffin, W.R., Johnson, P.R. and Abdelsalam, M.G., 2006a. From Island Arc to Craton: Timescales of Crustal Formation along the Neoproterozoic Bi'r Umq Suture Zone, Kingdom of Saudi Arabia, Saudi Geological Survey.
HargroveIII, U.S., Stern, R.J., Kimura, J.-I., Manton, W.I. and Johnson, P.R., 2006b. How juvenile is the Arabian-Nubian Shield? Evidence from Nd isotopes. Earth and Planetary Science Letters, 252: 308-326.
Hawkesworth, C.J. and Kemp, A.I.S., 2006. Evolution of the continental crust. Nature, 443: 811-817.
Jacobsen, S. and Pimentel-Klose, M., 1988. Nd isotopic variations in Precambrian banded iron formations. Geophysical Research Letters, 15: 393-396.
Jarrar, G., Saffarini, G., Baumann, A. and Wachendorf, H., 2004. Origin, age and petrogenesis of Neoproterozoic composite dikes from the Arabian-Nubian Shield, SW Jordan. Geological Journal, 39: 157-178.
Jarrar, G., Stern, R.J., Saffarini, G. and Al-Zubi, H., 2003. Late- and post-orogenic Neoproterozoic intrusions of Jordan: implications for crustal growth in the northernmost segment of the East African Orogen. Precambrian Research, 123: 295-320.
Jarrar, G.H., Wachendorf, H. and Zellmer, D., 1991. The Saramuj Conglomerate: Evolution of a Pan-African molasse sequence from southwest Jordan. N. Jb. Geol. Paleontol. Mn., 6: 335-356.
Johnson, P.R., 2003. Post-amalgamation basins of the NE Arabian shield and implications for Neoproterozoic III tectonism in the northern East African orogen. Precambrian Research, 123: 321-338.
Johnson, P.R., Kattan, F.H. and Al-Saleh, A.M., 2004. Neoproterozoic ophiolites in the Arabian Shield: Field relations and structure. In: T.M. Kusky (Editor), Precambrian Ophiolites and Related Rocks. Developments in Precambrian Geology. Elsevier, pp. 129-162.
Johnson, P.R. and Woldehaimanot, B., 2003. Development of the Arabian-Nubian Shield: Perspectives on accretion and deformation in the East African Orogen and the assembly of Gondwana. In: M. Yoshida, B.F. Windley and S. Dasgupta (Editors), Proterozoic East Gondwana: Supercontinent Assembly and Breakup. Geological Society, London, Pecial Publication, London, pp. 289-325.
Katzir, Y. et al., 2007 in press. Petrogenesis of A-type granites and origin of vertical zoning in the Katherina pluton, Gebel Mussa (Mt. Moses) area, Sinai, Egypt. Lithos.
Katzir, Y. et al., 2007. Interrelations between coeval mafic and A-type silicic magmas from composite dykes in a bimodal suite of southern Israel, northernmost Arabian-Nubian Shield: Geochemical and isotopic constraints.
Kennedy, A., Johnson, P.R. and Kattan, F.H., 2004. SHRIMP geochronology in the northern Arabian Shield. Part I: Data acquisition. Saudi Geological Survey Open File Report, SGS-OF-2004-11.

Kessel, R., Stein, M. and Navon, O., 1998. Petrogenesis of late Neoproterozoic dikes in the northern Arabian-Nubian Shield: Implications for the Origin of A-type granites. Precambrian Research, 92: 195-213.

Khalil, S.M. and McClay, K.R., 2002. Extensional fault-related folding, northwestern Red Sea, Egypt. Journal of Structural Geology, 24: 743-762.

Khudeir, A.A. and Asran, H.A., 1992. Back-arc Wizr ophiolites at Wadi Um Gheig District, Eastern Desert. Bulletin Faculty of Science, Assiut University, 21(2-F): 1-22.

Kolodner, K. et al., 2006. Provenance of north Gondwana Cambrian-Ordovician sandstone: U-Pb SHRIMP dating of detrital zircons from Israel and Jordan. Geological Magazine, 143(3): 367-391.

Kröner, A. et al., 1991. Evolution of Pan-African island arc assemblages in the southern Red Sea Hills, Sudan, and in southwestern Arabia as examplified by geochemistry and geochronology. Precambrian Research, 53: 99-118.

Kröner, A., Todt, W., Hussein, I.M., Mansour, M. and Rashwan, A.A., 1992. Dating of late Proterozoic ophiolites in Egypt and Sudan using the single grain zircon evaporation technique. Precambrian Research, 59: 15-32.

Loizenbauer, J. et al., 2001. Structural geology, single zircon ages and fluid inclusion studies of the Meatiq metamorphic core complex: Implications for Neoproterozoic tectonics in the Eastern Desert of Egypt. Precambrian Research, 110: 357-383.

Meert, J.G., 2003. A synopsis of events related to the assembly of eastern Gondwana. Tectonophysics, 362: 1-40.

Miller, N. et al., 2003. Significance of the Tambien group (Tigrai, N. Ethiopia) for Snowball Earth events in the Arabian-Nubian Shield. Precambrian Research, 121: 263-283.

Moghazi, A.-K.M., 1999. Geochemical and Sr-Nd-Pb isotopic data bearing on the origin of Pan-African granitoids in the Kid area, southeast Sinai, Egypt. Journal of the Geological Society, London, 155: 285-300.

Moghazi, A.M., 2003. Geochemistry and petrogenesis of a high-K calc-alkaline Dokhan Volcanic suite, South Safaga area, Egypt: the role of late Neoproterozoic crustal extension. Precambrian Research, 125: 161-178.

Mohamed, F.H., Moghazi, A.M. and Hassanen, M.A., 2000. Geochemistry, petrogenesis and tectonic settingof late Neoproterozoic Dokhan-type volcanic rocks in the Fatira area, eastern Egypt. International Journal of Earth Sciences, 88(764-777).

Moussa, E.M.M., Stern, R.J., Manton, W.I. and Ali, K.A., submitted. SHRIMP Zircon Dating and Sm/Nd isotopic investigations of Neoproterozoic granitoids, Eastern Desert, Egypt: No Evidence for pre-Neoproterozoic crust. Precambrian Research.

Nassief, M.O., Macdonald, R. and Gass, I.G., 1984. The Jebel Thurwah upper Proterozoic ophiolite complex, western Saudi Arabia. J. Geological Society, London, 141: 537-546.

Neumayr, P. and Khudeir, A.A., 1998. The Meatiq dome (Eastern Desert, Egypt) a Precambrian metamorphic core complex: petrological and geological evicence. Journal of Metamorphic Geology, 16: 259-279.

Pallister, J.S., Stacey, J.S., Fischer, L.B. and Premo, W.R., 1988. Precambrian ophiolites of Arabia: Geologic settings, U-Pb geochronology, Pb-isotope characteristics, and implications for continental accretion. Precambrian Research, 38: 1-54.

Pearce, J.A., 2003. Supra-subduction Zone Ophiolites: The Search for Modern Analogues. In: Y. Dilek and S. Newcomb (Editors), Ophiolite Concept and the Evolution of Geological Thought. Geological Society of America Special Paper, Boulder, pp. 269-293.

Ries, A.C., Shackleton, R.M., Graham, R.H. and Fitches, W.R., 1983. Pan-African structures, ophiolites and mélange in the Eastern Desert of Egypt: A traverse at 26°N. Journal of the Geological Society of London, 140: 75-95.

Rittmann, A., 1958. Geosynclinal volcanism, Ophiolites and Barramiya rocks. The Egyptian Journal of Geology, 2: 61-66.

Schürmann, H.M.E., 1966. The Pre-Cambrian along the Gulf of Suez and the northern part of the Red Sea. E. J. Brill, Leiden, 404 pp.

Shackleton, R.M., Ries, A.C., Graham, R.H. and Fitches, W.R., 1980. Late Precambrian ophiolitic mélange in the Eastern Desert of Egypt. Nature, 285: 472-474.

Shalaby, A. et al., 2005. The Wadi Mubarak belt, Eastern Desert of Egypt: A Neoproterozoic conjugate shear system in the Arabian-Nubian Shield. Precambrian Research, 136(1): 27-50.

Sims, P.K. and James, H.L., 1984. Banded iron-formations of late Proterozoic age in the central Eastern Desert, Egypt; geology and tectonic setting. Economic Geology, 79: 1777-1784.

Stein, M. and Goldstein, S., 1996. From plume head to continental lithosphere in the Arabian-Nubian Shield. Nature, 382: 773-778.

Stern, R.J., 1979. Late Precambrian Ensimatic Volcanism in the Central Eastern Desert of Egypt, UC San Diego, La Jolla CA, 210 pp.

Stern, R.J., 1981. Petrogenesis and tectonic setting of late Precambrian ensimatic volcanic rocks, Central Eastern Desert of Egypt. Precambrian Research, 16: 195-230.

Stern, R.J., 1985. The Najd Fault System, Saudi Arabia and Egypt: A Late Precambrian rift-related transform system? Tectonics, 4: 497-511.

Stern, R.J., 1994. Arc assembly and Continental Collision in the Neoproterozoic East African Orogen: Implications for the Consolidation of Gondwanaland. Annual Reviews of Earth and Planetary Sciences, 22: 319-351.

Stern, R.J., 2002. Crustal evolution in the East African Orogen: a neodymium isotopic perspective. Journal of African Earth Sciences, 34: 109-117.

Stern, R.J., 2004. Subduction initiation: Spontaneous and Induced. Earth and Planetary Science Letters.

Stern, R.J., Avigad, D., Miller, N.R. and Beyth, M., 2006. Evidence for the Snowball Earth hypothesis in the Arabian-Nubian Shield and the East African Orogen. Journal of African Earth Sciences, 44: 1-20.

Stern, R.J. and Gottfried, D., 1986. Petrogenesis of a Late Precambrian (575-600 Ma) bimodal suite in the North Eastern Desert of Egypt. Contributions to Mineralogy and Petrology, 92: 492-501.

Stern, R.J., Gottfried, D. and Hedge, C.E., 1984. Late Precambrian rifting and crustal evolution in the Northeastern Desert of Egypt. Geology, 12: 168-171.

Stern, R.J. and Gwinn, C.J., 1990. Origin of Late Precambrian Intrusive Carbonates, Eastern Desert of Egypt and Sudan: C, O, and Sr Isotopic Evidence. Precambrian Research, 46: 259-272.
Stern, R.J. and Hedge, C.E., 1985. Geochronologic constraints on late Precambrian crustal evolution in the Eastern Desert of Egypt. American Journal of Science, 285: 97-127.
Stern, R.J., Johnson, P.J., A. Kröner and Yibas, B., 2004. Neoproterozoic Ophiolites of the Arabian-Nubian Shield. In: T. Kusky (Editor), Precambrian Ophiolites. Elsevier, Amsterdam.
Stern, R.J. et al., 1990. Orientation of late Precambrian sutures in the Arabian-Nubian shield. Geology, 18: 1103-1106.
Stern, R.J., Sellers, G. and Gottfried, D., 1988. Bimodal dike swarms in the Northeast Desert of Egypt: Significance for the origin of late Precambrian 'A-Type' granites in northern Afro-Arabia. In: R. Greiling and S.E. Gaby (Editors), The Pan-African belt of NE Africa and Adjacent areas: Tectonic Evolution and Economic Aspects, pp. 147-179.
Stern, R.J. and Voegeli, D.A., 1987. Geochemistry, geochronology, and petrogenesis of a late Precambrian (~590 Ma) composite dike from the North Eastern Desertof Egypt. Geol. Rundschau, 76: 325-341.
Stoeser, D.B. and Frost, C.D., 2006. Nd, Pb, Sr, and O isotopic characterization of Saudi Arabian Shield terranes. Chemical Geology, 226: 163-188.
Stoeser, D.B., Whitehouse, M.J. and Stacey, J.S., 2001. The Khida Terrane - Geology of Paleoproterozoic Rocks in the Muhayil Area, Eastern Arabian Shield, Saudi Arabia (extended abstract). Gondwana Research, 4(2): 192-194.
Sturchio, N.C., Sultan, M. and Batiza, R., 1983. Geology and origin of Meatiq Dome, Egypt; a Precambrian metamorphic core complex? Geology, 11: 72-76.
Sultan, M., Arvidson, R.E., Duncan, I.J., Stern, R.J. and Kaliouby, B.E., 1988. Extension of the Najd shear system from Saudi Arabia to the central Eastern Desert of Egypt based on integrated field and Landsat observations. Tectonics, 7: 1291-1306.
Sultan, M. et al., 1990. Geochronologic and isotopic evidence for the involvement of pre-Pan-African crust in the Nubian shield, Egypt. Geology, 18: 761-764.
Surour, A.A. and Arafa, E.H., 1997. Ophicarbonates: calichified serpentinites from Gebel Moghara, Wadi Ghadir area, Eastern Desert, Egypt. Journal of African Earth Sciences, 24: 315-324.
Whitehouse, M.J., Stoeser, D.B. and Stacey, J.S., 2001. The Khida Terrane - Geochronological and Isotopic Evidence for Paleoproterozoic and Archean Crust in the Eastern Arabian Shield of Saudi Arabia (extended abstract). Gondwana Research, 4(2): 200-202.
Wilde, S.A. and Youssef, K., 2000. Significance of SHRIMP U-Pb dating of the Imperial Porphyry and associated Dokhan Volcanics, Gebel Dokhan, north Eastern Desert, Egypt. J. African Earth Sci., 31: 403-413.
Wilde, S.A. and Youssef, K., 2002. A re-evaluation of the origin and setting of the Late Precambrian Hammamat Group based on SHRIMP U-Pb dating of detrital zircons from Gebel Um Tawat, North-Eastern Desert. Journal Geol. Soc. London, 159: 595-604.

Willis, K.M., Stern, R.J. and Clauer, N., 1988. Age and Geochemistry of Late Precambrian Sediments of the Hammamat Seris from the Northeastern Desert of Egypt. Precambrian Research, 42: 173-187.

Zimmer, M., Kroner, A., Jochum, K.P., Reischmann, T. and Todt, W., 1995. The Gabal Gerf complex: A Precambrian N-MORB ophiolite in the Nubian Shield, NE Africa. Chemical Geology, 123: 29-51.

Zoheir, B.A. and Klemm, D.D., 2006 in press. The tectono-metamorphic evolution of the central part of the Neoproterozoic Allaqi-Heiani suture, south Eastern desert of Egypt. Gondwana Research.

Appendix 1

Via Porphyrites
This article appeared on pages 2-9 of the November/December 1998 print edition of Saudi Aramco World.
Written by Louis Werner

In the year 18, in Egypt, a Roman legionnaire named Caius Cominius Leugas found a type of stone he had never seen before. It was purple, flecked with white crystals and very fine-grained. The latter characteristic made it excellent for carving, and it became an imperial prerogative to quarry it, to build or sculpt with it, or even to possess it. This stone soon came to symbolize the nature of rulership itself. We call it imperial porphyry.

The Romans used this porphyry for the Pantheon's inlaid panels, for the togas in the sculpted portraiture of their emperors, and for the monolithic pillars of Baalbek's Temple of Heliopolis in Lebanon. Today there are at least 134 porphyry columns in buildings around Rome, all reused from imperial times, and countless altars, basins and other objects.

Byzantium, too, was enamored of porphyry. Constantine the Great celebrated the founding of his new capital, Constantinople (later Istanbul), in the year 330 of our era by erecting there a 30-meter (100') pillar, built of seven porphyry drums, or cylinders, that still stands. Eight monolithic columns of porphyry support Hagia Sophia's exedrae, or semicircular niches. Justinian's chronicler, Procopius, called the columns "a meadow with its flowers in full bloom, surely to make a man marvel at the purple of some and at those on which the crimson glows."

Anna Comnena, daughter of the 11th-century emperor Alexius I, described the porphyra, a porphyry-veneered room in the palace where women of the ruling family were taken to give birth. The choice of porphyry for this room in particular was no accident: It ensured that members of the imperial family were literally porphyrogenitos, or "born to the purple."

The room is in the form of a perfect square from floor to ceiling, with the letter ending in a pyramid. The stone used was of a purple color throught with white spots like sand sprinkled over it.

Porphyry served the imperium in death as well as birth. Nero was the first emperor to be entombed in a porphyry sarcophagus, according to Suetonius. Constantine's porphyry sarcophagus has been lost, but that of his wife Constantia, decorated with peacocks, lambs, and grapes and thought to be a copy of his, is now in the collection of the Vatican Library. Those of the Holy Roman Emperors Frederick II, Henry IV and William I, and that of the Empress Constance, all porphyry, are in Sicily's Palermo and Monreale cathedrals.

In later centuries, porphyry columns and other pieces were widely reused in new constructions, often reappearing far from their original Roman context. In 786, Charlemagne received permission from Pope Hadrian to remove classical columns of porphyry from Rome to build his cathedral at Aachen. The renaissance Medici family commissioned portrait busts carved from porphyry blocks that had been warehoused in

Rome since imperial times. Other sources are unknown and unguessable: The Victoria and Albert Museum in London contains a pair of fine porphyry earrings. A church in Kiev is decorated with porphyry wall and floor revetments; how the stone made its way there is probably an interesting story, but unrecorded.

What makes imperial porphyry so precious and rare is that it is found at only one place on earth, atop a 1600-meter (mile-high) mountain in the eastern province of Egypt. The Romans named the site Mons Porphyrites, or Porphyry Mountain, and the Arabs today call it Jabal Abu Dukhan, or Smoky Mountain.

Thrust to the earth's surface in the same volcanic action that once formed the Red Sea, the porphyry found at Mons Porphyrites is, as far as specialists know, geologically unique. But the site is so barren and so remote that only slave labor could ever have extracted the stone, and even then only for the relatively brief historical moment when Roman power was at its zenith.

When George Murray, chief of the Egyptian Geographical Survey in the 1930's, visited the quarry, he found a place so barren that it made him shudder. A ruined fortress, three lifeless villages, abandoned temples and shrines, dry wells, broken pillars, cracked stone baths—"the fossil whims of three centuries of Emperors," he called it. The local Ma'aza Bedouin have a similar saying about the place: "The Romans left; only the ibex remained."

But geographers and Bedouin see things differently from archeologists. David Peacock of the University of Southampton in England is co-director of the Egypt Exploration Society's Mons Porphyrites Project, and he finds it "the most remarkable Roman industrial landscape in the world." Some of his recent finds, including the stela inscribed by the Roman discoverer of the quarry, help to explain how the work was carried out under conditions that would be daunting even today.

Among the more startling finds are a hair-pin, cosmetic brush, and toy comb made from oyster shell—evidence that women and children may have lived here alongside the men. Also surprising is written evidence, on inscribed pottery shards, or ostraca, that work proceeded here even during the sun-scorched summer.

Labor involved more than mere quarrying. After cutting and rough-dressing the blocks and column drums—and apparently also such larger pieces as the monolithic pillars eventually used in Hagia Sophia—the pieces were loaded onto oxcarts, which were driven 150 kilometers (about 100 mi) to the Nile at Qena (Kainopolis of the Ptolemaic era), where they were shipped downstream by barge and then by sea to their final destinations. Byzantine poet Paul Silentarius refers to this in his ode to Constantinople's porphyry, "powdered with bright stars, that has laden the river-boat on the broad Nile."

The road from the quarry westward to Qena, which Ptolemy the Geographer put on his second-century map, was a route described first by Strabo, and it is to this day known as the Via Porphyrites, the Porphyry Road. Along the way are seven hydreumata, or fortified wells, each one a day's march from the next. Outside the fortifications are lines of large stones to which oxen were tethered at night.

Archeologist Steven Sidebotham of the University of Delaware, an authority on the Roman roads of the Red Sea mountains, surveyed the Via Porphyrites in 1989. He concluded that from the first to the third centuries of our era, the hydreumata were used as watering stations for the porphyry carts, and that in the following three centuries, when

quarrying had ceased and tribal raiding from the south had commenced, they became Roman border posts and strong points along the line of communication between the Nile and the fort at Abu Sha'ar on the Red Sea coast.

Today the area is uninhabited except for the occasional Ma'aza Bedouin grazing his camels. Ibex, hyrax, and rabbit live here now. Around water holes, trumpeter bullfinches, desert larks, and mourning chats flock in sayaal trees (Acacia raddiana) and the wispy-needled yasar trees (Moringa peregrina).In the fall, thousands of white storks cross overhead, riding thermal currents on their way from the Sinai to central Africa. The Via Porphyrites follows three major systems of wadis, or streambeds: Wadi Belih, Wadi al-Attrash and Wadi Qena. Between the first two it crosses the divide between the Red Sea watershed and that of the Nile. From Wadi Belih, there are two approaches to the quarry. One is a winding route up Wadi Umm Sidri and into Wadi Abu Mu'amal ("Workplace Wadi"), and it is this route that the oxcarts followed. The other is a steep but more direct footpath over a 950-meter (3000') pass.

A late-winter trek along the route in the company of two Ma'aza Bedouin, 72-year-old Salaama Mir'i and his 18-year-old son Suleiman, provides ample opportunity to reflect on the hardships faced nearly 2000 years ago by Rome's mostly Christian slaves, the thousands damnati ad metalla, or "condemned to the mines" in Egypt.

In walking to Mons Porphyrites, I follow in the footsteps of two British explorers, Sir John Wilkinson, a former president of the Royal Geographical Society, who rediscovered the quarry in 1823, and Leo Tregenza, a Qena-based schoolteacher who, in the 1940's, spent his summers in these parts and wrote of them in his classic account The Red Sea Mountains of Egypt (Oxford University Press, 1955).

When I tell Salaama of my intended route, he startles me by saying, "Yes, I know it, I came this way years ago with an ingilizi named Genza." "Leo Tregenza?" I ask. "Yes," he says, "A man always writing in a book, with many tins of bully beef and cocoa." When I later telephone Tregenza, now well into his 90's and living in Wales, he says, "There is not a day that goes by that I don't think of those men. Tell them that when you see them next."

Salaama dispatches his son to guide me up the quarry footpath north from our first camp in Wadi Mu'allaq, the Hanging Wadi, which cuts into the mountain on the other side of the summit from the old quarry. From the pass into Wadi Abu Mu'amal the view sweeps from the present to the ancient past: To the southeast, the white hotels of the booming resort town of Hurghada rise off the coastal plain. To the southwest floats Jabal Qattar, a massif of Precambrian red granite, and just beyond is Jabal Shayyib, at 2242 meters (7175') Egypt's highest point outside the Sinai Peninsula.

Looking north along the wadi floor, the remains of the stone fort and the Temple of Serapis are visible. Five white-plastered stone pillars surround the well. The temple has largely fallen, but the dedicatory inscriptions are still legible on the lintels that lie scattered on the ground. "Built when Rammius Martialis was governor of Egypt," Tregenza translated from one, which dates the temple to between the years 117 and 119. Out of sight around the corner is Wadi Umm Sidri's well, five meters (16') in diameter and once covered by an octagonal loggia. Nearby are four symmetrical crown-of-thorn trees (*Zizyphus spina-christi*) which Tregenza regarded as old enough to have been planted by the Romans for their shade. Further down the wadi is the great stone ramp where the porphyry blocks were loaded off quarry skids and onto long-distance carts.

One can only wonder how such heavy loads were managed. At the nearby white-granite quarry of Mons Claudianus lies a 22-meter (70'), 240-ton column, abandoned presumably when it cracked while being rough-dressed into an approximation of its final shape. Smaller columns there—so many that the Ababda Bedouin call the place "Mother of Pillars"—are in the same condition, which makes one think that for the Romans, shipping large monoliths out of these mountains was a relatively routine task.

Looking some 500 meters (1600') uphill, at the end of the myriad slipways running up the mountain's two facing flanks, are the angled faces of the porphyry quarries, which appear to have plenty of the stone left for the taking. The two-meter (6'), 20-ton blocks and drums were lowered down these steep, smoothed and banked slipways, restrained only by the blocks and tackle attached to paired stone butts set at close intervals on either side of each slipway, all along their length.

Here, too, are the lodging huts, watchmen's posts, blacksmiths' benches and dipping baths, the rock-hewn cisterns, the rubbish dumps and even the rough gravesites that all testify to everyday life against all odds. Tregenza recorded his find of one tombstone, made of porphyry, that belonged to "John of Hermopolis," presumably a Christian slave.

Earlier British visitors found improbable inspiration in this desolation. Poet and amateur archeologist Christopher Scaife, when not documenting Roman epigraphy in the area, was known to prance about the Temple of Serapis dressed in a blue toga. Tregenza himself found poetry in the color of the porphyry scree, seeing in it "a lurking bloom linked to the softness of the sky and the fine blue mist that descends from it."
But for me, there are only heat, dust and sharp stones that cut my boots. I am glad when I arrive back in camp after a six-hour return trip from the quarry. As twilight falls around our campfire, Suleiman makes unleavened bread under the coals, cleaning it with a whisk of ripped shirting before we dip our pieces into a bowl of melted samna (ghee, or clarified butter). Beyond, the lights of Hurghada blink, and the pack camels nose closer for the night.

The next morning we begin our trek toward the Nile. Badi'a is the first hydreuma along the route. Like the others, it measures roughly 14 square meters (150 sq ft) with interior rooms, in ruins but still unexcavated. The well itself has long ago drifted full of sand. The corner towers have fallen into cones of stone linked by the graceful undulations of the more intact two-meter (6') walls. Recent surface finds by Peacock include coins from the reigns of Hadrian, Trajan, Constantine and Theodosius, as well as pot- and glass shards.

An ostracon found nearby hints at how the coins might have arrived. "To Dionysius my most dear friend," it reads. "I ask that you send the money if you are able. Send it with Serapion since I need it, and do not fail. Goodbye." The writer's name is broken off the shard, so we will never know who had such a pressing need for money in a place where, it would seem, money could buy nothing.

The westward march from Badi'a moves between Jabal Qattar's red granite massif on the left and Abu Dukhan's black basalt on the right, the two hills placed like navigational buoys on a river. This stretch is still in the Red Sea watershed, so the gentle slope is against us until we top a pass some 250 meters higher than the point where the oxcarts would have begun their journey, just before the next hydreuma at the mouth of Wadi Qattar.

The well at this station was renovated by Egypt's Prince Farouk in the 1930's, and the Roman walls are now destroyed. Farouk quarried porphyry briefly, and used it to provide Cairo's modern building entries with their distinctive purple lintels. But his efforts lasted only long enough to relearn how hard the work was. Since then, the only modern quarrier was one Lady Cowdray, wife of a Scottish oil magnate, who had promised her husband he would be buried in a porphyry sarcophagus—and so he was.

A twisting, refreshingly shady side route winds through the ever-narrowing Wadi Qattar, past prehistoric drawings of ibex, giraffe, and sickle-boats, into the heart of the massif and up to a place known as Wadi Naqaat, or the Dripping Wadi. The sand here is pink, eroded from the quartz and felsites that make up the summits. An old Bedouin lion trap, enclosed in stone, with a tipping rock to shut the gate, sits on a low bluff.

Sir John Wilkinson's description of the wadi, published in the 1832 Journal of the Royal Geographical Society, remains accurate. "A mountain torrent's bed," he called it, "filled with large stones until it terminates at a precipitous rock overgrown with hanging water weeds, down which the water drops into a basin of plentiful supply."

Naqaat was home to a Christian anchorite community—founded perhaps by runaway slaves from Mons Porphyrites—and the hermits' fourth-century rock church remains in perfect condition, except for a missing roof. An inscription, now removed to Cairo, shows that it was built by Flavius Julius when Hatres was Bishop of Maximianopolis—the Roman name for modern Qena—a statement that dates it to the year 339 of our era.

In a fifth-century history of Christian hermits written by Palladius, one can read the first-person account of a man named Posidonius:

Living in the porphyry district for a year I met no man nor heard a voice nor tasted bread, keeping myself alive on dates and wild honey. Once these things failed me and I decided to go back to the world of man, but walking out I spied a Roman and in fright returned to my cave. On my way I came upon a basket of fresh figs, which overjoyed me and lasted for two months.

Four fig trees still grow next to Wadi Naqaat's pool. Ibex prints cross the mud bank, and moss and maidenhair ferns hang from the dripping wall. The water level, raised by the torrential rains three months before my passing, has receded slightly, but Salaama assures me that this is indeed a perennial source.

The entire wadi has apparently been well-watered by the rain. Slightly lower, a yasar tree is covered with tiny white blossoms, and mountain mallow plants (Malva parviflora) and humaad, with its edible red flowers, grow everywhere. We gather some mallow; it will add texture and freshness, if not much flavor, to the mostly tinned meals that will sustain us on our trip.

The way from Qattar to Deir al-Attrash, the next station, often follows in the old automobile tracks left from the 1930's, before the building of the asphalted Qena-Safaga road, when this was the principal crossing from the Nile to the sea. The tall Roman cairns placed in the middle of the wadi floor seem unnecessary as route markers, a fact that led archeologist Sidebotham to suggest that they were signal towers for flags or mirrors, for there is an unimpeded line of sight from one to the next.

Outside Deir al-Attrash's mud-brick walls lie several broken porphyry drums and blocks that apparently fell off their wagons. Out here, far from their loading ramps, the

Roman carters had no way of putting them back onto a cart again, and thus had no option but to leave them behind, where they are slowly eroding to nothing, their purple chips and sands becoming lost among the dull schists and diorites that dominate these low foothills.

The tributary wadis entering from Jabal Qattar's western flanks are broader thanthose that slice into the higher peaks. As we approach the mouth of Wadi al-Attrash, a herd of 13 loose camels wanders up to us. "Many different brands," notes Salaama from a distance, "but all Khushmaani," referring to a Ma'aza clan that rivals his own Masaari lineage.

We pass the turnoff to Mons Claudianus and, high on an outcrop, see another ruined hydreuma with walled guard posts. The route soon squeezes through the landmark Bab al-Mukheniq, the Gate of Suffocation, formed by two high granite ridges, before entering the gravel plain known as Naq' al-Tayr, or Bird Swamp. Just as the march begins in earnest, across to the long bluff that drops off into Wadi Qena, I ask myself, "Where is the swamp—and where are the birds?"

The watery mirage shimmering across the plain answers the first question, and Tregenza takes care of the second. As he witnessed in the fall of 1949, this is where migrating storks by the thousands land to rest, fooled perhaps by the same false promise of a drink that I too had momentarily believed.

The flat limestone plateau that separates the Nile Valley from the wadi system we are in provides a straight-edged horizon, in contrast to the craggy, igneous teeth of the mountains now at our backs. The Wadi Qena is broad and hot, crisscrossed with the ruts of joyriding jeeps, but the soft rays of the setting sun illuminate a fainter trace in the firm sand: Roman cart tracks.

The three-meter-wide (10') tracks spread out all across the plain, running in sets of two parallel lines, as if this had been a proving ground for racing chariots. The tracks are almost imperceptible when we look directly down; they can best be seen by standing in the middle of a set and gazing along them toward the horizon. In some low spots where rainfall has collected they are easier to see, because grass grows in their double wheel-tracks and nowhere else.

Many of the tracks lead to the hydreuma of Saqqia, built on a low hill beside the plain. At the center of its earthen berm perimeter are two wide wells which once fed the upper-level animal troughs and cisterns with water lifted by shadouf the ancient Egyptian counterbalanced water-lifting device. Seashells dot the ground; they were used to make the lime plaster that still coats the troughs. The odd porphyry chip or blue faience shard turns up with a kick at the dirt.

Al-Heita, the penultimate hydreuma, has a double fort, one in the wadi bed next to a rare stretch of paved Roman road, and the other high on a shoulder of Jabal Abu Had, which is a limestone shelf at Wadi Qena's eastern limit. The yellow brick of the fort's upper walls, showing the remains of finely executed barrel vaults, are a beautiful and conspicuous ruin against the sky.

It was here that Tregenza found a Roman love letter written on an ostracon. "From Isadora to her lord and master, greetings. As I begged you before, please do not forget me. I want you to send the bottle and ink so I may write to you again." Here was additional evidence that Roman women, too, once traversed these desiccated parts.
It was here I had to leave Salaama and Suleiman. I would have to miss the last water

station—which is said to be completely ruined—and take a truck down to Qena, where Rome's presence still resonates in the magnificent Temple of Denderah— a temple which, ironically, lacks any sign of porphyry decoration.

The two Ma'aza will return with the camels past Mons Porphyrites to their home range in the Wadi Umm Duheis above Hurghada. I wonder if they, like Isadora, might also leave a record somewhere of this journey. If they do, I would hope it will not resemble the message on papyrus recently found in the Fayoum, west of the Nile between Qena and Cairo. That was written in the year 163, 18 centuries ago, by Satabous of Dimai, and in it he complained bitterly that his camels had been unfairly requisitioned by the authorities—for "draft service on the porphyry road."

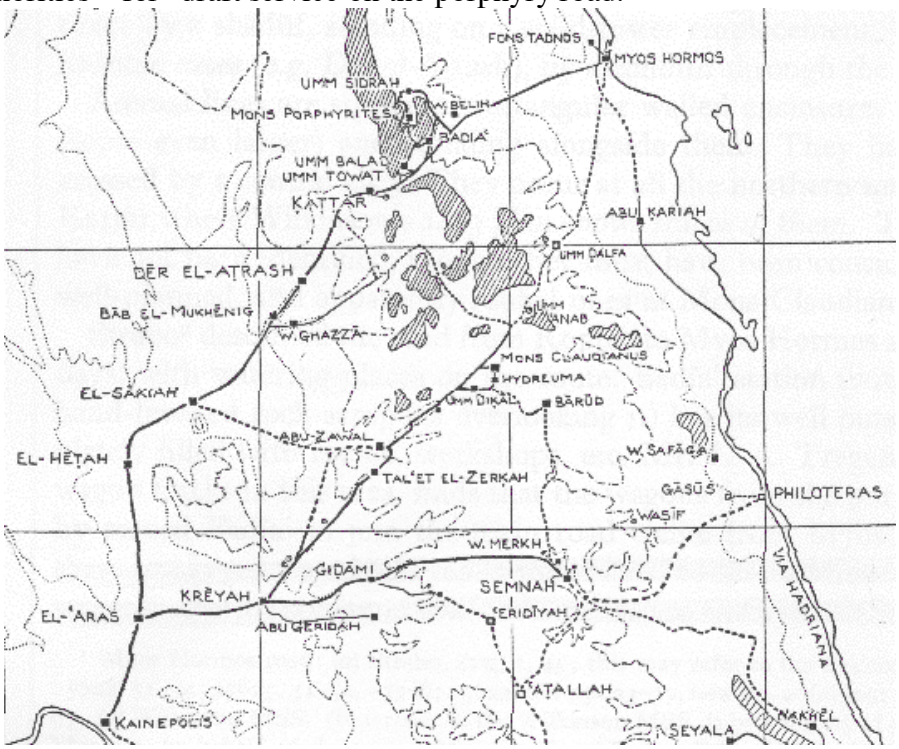

Map of the Roman roads running through the Eastern Desert, major habitations labeled with squares, the Nile in the bottom-left corner of the map, the Red Sea to the far right, and Mons Porphyrites indicated with a box. From Meredith (1952).